2021-12

ELECTROMAGNETIC COMPATIBILITY DESIGN AND TEST FOR MEGAWATT MEDIUM VOLTAGE SOLID STATE CIRCUIT BREAKER

Everhart, Zachary J.

Monterey, CA; Naval Postgraduate School

NAVAL POSTGRADUATE SCHOOL

MONTEREY, CALIFORNIA

THESIS

ELECTROMAGNETIC COMPATIBILITY DESIGN AND TEST FOR MEGAWATT MEDIUM VOLTAGE SOLID STATE CIRCUIT BREAKER

by

Zachary J. Everhart

December 2021

Thesis Advisor: Di Zhang
Co-Advisor: Giovanna Oriti

THIS PAGE INTENTIONALLY LEFT BLANK

REPORT DOCUMENTATION PAGE	*Form Approved OMB No. 0704-0188*

1. AGENCY USE ONLY *(Leave blank)*	**2. REPORT DATE** December 2021	**3. REPORT TYPE AND DATES COVERED** Master's thesis

4. TITLE AND SUBTITLE
ELECTROMAGNETIC COMPATIBILITY DESIGN AND TEST FOR MEGAWATT MEDIUM VOLTAGE SOLID STATE CIRCUIT BREAKER

5. FUNDING NUMBERS
REP3L

6. AUTHOR(S) Zachary J. Everhart

7. PERFORMING ORGANIZATION NAME(S) AND ADDRESS(ES)
Naval Postgraduate School
Monterey, CA 93943-5000

8. PERFORMING ORGANIZATION REPORT NUMBER

9. SPONSORING / MONITORING AGENCY NAME(S) AND ADDRESS(ES)
NASA Glen Research Center 21000 Brookpark Rd, Cleveland, OH 44135

10. SPONSORING / MONITORING AGENCY REPORT NUMBER

11. SUPPLEMENTARY NOTES The views expressed in this thesis are those of the author and do not reflect the official policy or position of the Department of Defense or the U.S. Government.

12a. DISTRIBUTION / AVAILABILITY STATEMENT
Approved for public release. Distribution is unlimited.

12b. DISTRIBUTION CODE
A

13. ABSTRACT (maximum 200 words)

Naval Postgraduate School and the Naval Surface Warfare Center Philadelphia Division, University of Connecticut, and Clemson University propose to advance the response speed, power density, efficiency, and altitude capability of circuit breaker technology by developing a fast lightweight altitude-ready solid state circuit breaker for hybrid electric propulsion (FLASH). This thesis describes the procedure and methods used to create a nondestructive testbed that identifies the potential issues in the circuit breaker related to electromagnetic interference (EMI) susceptibility. The testbed uses magnetic and electric field injection to simulate harsh EMI environments and pinpoints the exact areas within a system that are susceptible to EMI. Furthermore, this thesis recommends low-cost solutions to correct the identified problematic areas and components. Lastly, the testbed designed in this thesis can be used on the FLASH circuit breaker as well as a wide range of other applications and electrical circuits. This thesis will identify the potential issues in the circuit breaker related to EMI and proposes solutions that will help the team integrate the solutions in the circuit breaker design. In addition, it develops a tool used to enhance the EMI performance of the circuit breaker components. Lastly, this thesis documents the results of the full power test and validates the proposed solutions with experimental data.

14. SUBJECT TERMS
electromagnetic interference, EMI, megawatt medium voltage, solid state circuit breaker, electromagnetic compatibility design and test, fast light-weight altitude ready solid state circuit breaker for hybrid electric propulsion, FLASH, nondestructive, EMI susceptibility

15. NUMBER OF PAGES
97

16. PRICE CODE

17. SECURITY CLASSIFICATION OF REPORT	**18. SECURITY CLASSIFICATION OF THIS PAGE**	**19. SECURITY CLASSIFICATION OF ABSTRACT**	**20. LIMITATION OF ABSTRACT**
Unclassified	Unclassified	Unclassified	UU

NSN 7540-01-280-5500

Standard Form 298 (Rev. 2-89)
Prescribed by ANSI Std. 239-18

THIS PAGE INTENTIONALLY LEFT BLANK

Approved for public release. Distribution is unlimited.

ELECTROMAGNETIC COMPATIBILITY DESIGN AND TEST FOR MEGAWATT MEDIUM VOLTAGE SOLID STATE CIRCUIT BREAKER

Zachary J. Everhart
Lieutenant, United States Navy
BS, United States Naval Academy, 2015

Submitted in partial fulfillment of the
requirements for the degree of

MASTER OF SCIENCE IN ELECTRICAL ENGINEERING

from the

NAVAL POSTGRADUATE SCHOOL
December 2021

Approved by: Di Zhang
Advisor

Giovanna Oriti
Co-Advisor

Douglas J. Fouts
Chair, Department of Electrical and Computer Engineering

THIS PAGE INTENTIONALLY LEFT BLANK

ABSTRACT

Naval Postgraduate School and the Naval Surface Warfare Center Philadelphia Division, University of Connecticut, and Clemson University propose to advance the response speed, power density, efficiency, and altitude capability of circuit breaker technology by developing a fast lightweight altitude-ready solid state circuit breaker for hybrid electric propulsion (FLASH). This thesis describes the procedure and methods used to create a nondestructive testbed that identifies the potential issues in the circuit breaker related to electromagnetic interference (EMI) susceptibility. The testbed uses magnetic and electric field injection to simulate harsh EMI environments and pinpoints the exact areas within a system that are susceptible to EMI. Furthermore, this thesis recommends low-cost solutions to correct the identified problematic areas and components. Lastly, the testbed designed in this thesis can be used on the FLASH circuit breaker as well as a wide range of other applications and electrical circuits. This thesis will identify the potential issues in the circuit breaker related to EMI and proposes solutions that will help the team integrate the solutions in the circuit breaker design. In addition, it develops a tool used to enhance the EMI performance of the circuit breaker components. Lastly, this thesis documents the results of the full power test and validates the proposed solutions with experimental data.

THIS PAGE INTENTIONALLY LEFT BLANK

TABLE OF CONTENTS

LIST OF FIGURES

THIS PAGE INTENTIONALLY LEFT BLANK

LIST OF TABLES

THIS PAGE INTENTIONALLY LEFT BLANK

LIST OF ACRONYMS AND ABBREVIATIONS

AC	alternating current
BCI	bulk current injection
DOD	Department of Defense
DC	direct current
EM	electromagnetic
EMC	electromagnetic compatibility
EMF	electromotive force
EMI	electromagnetic interference
EUT	equipment under test
FLASH	fast light-weight altitude-ready solid state circuit breaker for hybrid electric propulsion
IGBT	insulated-gate bipolar transistor
MOSFET	metal oxide semiconductor field effect transistor
MOV	metal oxide varistor
MVDC	medium voltage DC
NASA	National Aeronautics and Space Administration
NAVIR-WD	Naval Air System Command Weapon Division
NEAT	NASA electric aircraft testbed
NSWCPD	Naval Surface Warfare Center Philadelphia Division
RF	radio frequency
T&E	test and evaluation
TEM	transverse electromagnetic
TRL	technology readiness level
VCC	voltage clamping circuit

THIS PAGE INTENTIONALLY LEFT BLANK

ACKNOWLEDGMENTS

First, I would like to thank Dr. Michael Schutten for his continued guidance and assistance. His expertise and ability to teach significantly helped me throughout the thesis process. Dr. Schutten spent several months mentoring and teaching me about EMI susceptibility and how we can make systems more robust. The knowledge I gained from working with Dr. Schutten will help me throughout the rest of my professional career.

Next, I would like to thank Professor Di Zhang. His constant help fostered my education while at Naval Postgraduate School. The information I learned from him will stick with me throughout my career.

Lastly, I would like to thank Professor Oriti for his continued help and direction. I sincerely enjoyed being one of his students and learned so much about power electronics. The help she provided throughout the thesis process elevated my thesis and improved my professional knowledge.

Again, thank you all for your support.

THIS PAGE INTENTIONALLY LEFT BLANK

I. INTRODUCTION

Electromagnetic interference (EMI) creates significant problems for electronic systems by disrupting the systems intended operation. These problems occur between electronic and electrical systems and have been documented and studied for decades. EMI susceptibility refers to the vulnerability of a system to electromagnetic energy radiated by another electronic or electrical system or device. Engineers do not want EMI emission or susceptibility issues to occur in their circuits, so they must design the system to reduce or prevent the effects of EMI from occurring. Critical systems on ships, aircraft, or spacecraft need to be designed, constructed, and tested to minimize the severity and impact of EMI. Reducing system EMI susceptibility and emissions will ensure long lasting and reliable operation.

A. SIGNIFICANCE OF RESEARCH

An effective nondestructive test platform is needed to efficiently test the electromagnetic compatibility (EMC) and robustness of electronic and electrical circuit boards and reduce their EMI susceptibility [1], [2]. Electronic and electrical systems have the ability to unintentionally radiate large magnetic or electric fields that can corrupt their own signals and nearby systems [3], [4]. Often, EMI is overlooked in the initial design phase and then the complete system experiences noise issues that can be difficult to troubleshoot and eliminate. This EMI noise can degrade the systems performance, reliability, and lifespan [1].

Existing EMI susceptibly testing consists of inducing large amounts of energy into the equipment under test (EUT), which often results in permanent damage to the electrical components being tested [5]. Naval Postgraduate School (NPS) is constructing a testbed to perform nondestructive EMI testing. This testing will ensure robust operation of the logic boards associated with the fast light-weight altitude-ready solid state circuit breaker for hybrid electric propulsion (FLASH) system. This thesis presents the testbed developed to test the FLASH logic board for EMI susceptibility problems and identify components that are susceptible to EMI failures. This EMI susceptibility testbed can be used to test electrical

circuits that may be exposed to a harsh EMI environment. After the testing described in this thesis is complete, the system can be redesigned to mitigate or eliminate the areas of the board that are electromagnetically weak [1], [5]. This removes the need for other more costly EMI corrective actions, such as filtering and shielding [5], [6].

Issues caused by EMI are becoming more relevant and costly throughout the U.S. military. The Navy is beginning to integrate new high power radar systems and electric drive ships into the fleet, resulting in new potential EMI issues [7]. The large amounts of power needed to operate these radars and propulsion plants can have adverse effects on themselves, other systems, and nearby vessels. For example, in June 2000 the minesweeper HMAS Huon lost control of its steering gear and nearly hit the frigate HMAS Anzac [8], [9]. As the two ships approached, the HMAS Anzac radars induced EMI into the HMAS Huon electronic steering control system, resulting in a total loss of control [8]. This example of a near-miss highlights the importance of proper design and testing of critical systems to ensure they are resilient to the effects of EMI. The Australian National Audit Office conducted a review of the incident and concluded a lack of proper test and evaluation (T&E) on both ships was the reason the two ships nearly collided [8], [9].

The work described in this thesis will show why testing electrical systems for EMI early in the design process is important, and more efficient and reliable than simply shielding components [1], [5]. Specifically, for components that will be installed on spacecraft and satellites, shielding is very heavy and costly, and can be improperly reworked, reducing its performance over time [10].

> In a new study published in Space Weather, researchers from the Massachusetts Institute of Technology (MIT) say that solar flares, geomagnetic storms and other forms of electromagnetic radiation may be to blame for up to 26 failures in eight geostationary satellites owned by London-based telecommunications company Inmarsat that took place over 16 years of operation… Designed to last for up to 15 years, the satellites are heavily shielded to protect sensitive electronic components from solar radiation; however, say MIT researchers, over time radiation can penetrate the shielding and affect the performance of these components… Results from the study indicated that the majority of the Inmarsat satellite failures overlapped with periods of high-energy electron activity during declining phases of the solar cycle. The researchers believe that this particle flux may have accumulated in the satellites over time, creating internal charging that

> damaged the amplifiers responsible for strengthening and relaying signals back to Earth. While most satellites carry back-up amplifiers, says Lohmeyer, over time this supply may run out. (Banana Skins 816, 2014) [9]

For electrical components installed on spacecraft, extra design and testing precautions must be taken to ensure components or subsystems do not become susceptible to EMI over time [10]. Therefore, the electrical components need to be designed and tested for EMI susceptibility with sufficient margin so reliance on shielding and filtering can be reduced or even eliminated.

The U.S. Navy has been severely impacted by EMI problems in the past [11]. In 1967, the tragic fire that occurred on the aircraft carrier USS Forrestal was caused by EMI, and resulted in the death of 134 Sailors and injury of 161 Sailors [11]. The massive fire was caused by the inadvertent ignition of a Zuni rocket that was carried on a F-4B Phantom aircraft. The Zuni rocket struck the fuel tank of a nearby A-4 Seahawk, causing jet fuel to be spilled all over the flight deck area. The official inquiry revealed a shipboard radar and degraded shielding on the Zuni rocket firing mechanism triggered the rocket to fire, initiating the incident [11], [12]. Since then, the Navy has revised it requirements and standards for EMI and explosive ordinance to prevent similar accidents from occurring.

The FLASH program and other Navy applications need a robust testing system that improves EMI susceptibility [7]. Traditional EMI susceptibility methods can damage the EUT and may not provide adequate system robustness [5]. EMI susceptibility problems have often been mitigated by using filtering and shielding [6], this is not a cost effective or practical solution for the FLASH program. This thesis describes the methods EMI can enter into a system, the procedure used to test for EMI susceptibility, and low-cost fixes that can be used to improve the system robustness.

B. RESEARCH PROBLEM SPACE

The Department of Defense (DOD) is concerned with EMI and EMC within solid-state circuit breakers because the next generation weapon systems and sensors require direct current (DC) power distribution and control as part of their integration into ship power systems. Protecting these systems and loads from unintentional electromagnetically

induced faults is crucial to ensure the operability and proper maintenance of vital loads during combat operations and conditions [10]. Therefore, there is an effort from the Naval Surface Warfare Center Philadelphia Division (NSWCPD) to develop a new family of solid state medium voltage DC (MVDC) circuit protection devices capable of providing the fault detection and response times needed for the next generation of DC power distribution systems. The circuit breaker being developed is a 1 kV, 1 kA DC circuit breaker with the clearing time less than 1 ms and a power density of 18 MW/m^3 and weighs 200 lbs [7]. The system has been developed and tested at TRL 5 at sea [7].

The Naval Postgraduate School, teamed with the Naval Surface Warfare Center Philadelphia Division (NSWCPD), Naval Air System Command Weapon Division (NAVIR-WD), University of Connecticut, Virginia Tech and Clemson University, proposes to advance the response speed, power density, EMI robustness, and altitude capability of circuit breaker technology by developing a fast light-weight altitude-ready solid state circuit breaker for hybrid electric propulsion (FLASH) system. The solid-state circuit breaker is based on mature and cost-effective Silicon (Si) insulated-gate bipolar transistors (IGBT), which must meet the following specifications:

- Block 2 kV
- Carry 1.2 kA continuously
- Higher than 99.5% efficiency
- Interrupt up to 5 kA current within 10 μs
- Power density greater than 100 kW/kg
- Limit the peak fault current to 5 kA
- Altitude operation condition of 35 kft or higher
- Operation up to 160° F coolant
- Technology readiness level (TRL) 6 and demonstration at NASA in 2023 (Note: TRL 6 is requires a system/subsystem model or prototype demonstration in a relevant environment)
- Scalable to 10 kV and 10 kA for future applications [7]

This effort to design and test FLASH will significantly improve upon the existing Navy 1kV, 1 kA dc circuit breaker technology to achieve the efficiency, power density, and altitude capability targets specified by NASA [7]. The FLASH solid state circuit breaker will be integrated in a full power demonstration using the NASA Electric Aircraft Testbed (NEAT) in 2023 [7].

The FLASH solid state circuit breaker needs logic circuit boards that are not susceptible to failure from the large electromagnetic transients during operation of the circuit breaker. The electronic circuits need to be designed, tested, and constructed to be robust in a severe EMI environment, ensuring reliable operation. Traditionally, only shielding and filtering have been used to protect electric circuits from EMI, but this adds additional weight and failure modes for the aircraft/spacecraft that will operate the FLASH hybrid propulsion system [5], [10]. As a result, extensive EMI testing is required to identify and correct electromagnetically weak points on the circuit boards, creating a robust system [1].

C. RESEARCH QUESTION

Can EMI susceptibility issues be identified with nondestructive near field testing on electrical systems and components?

D. APPROACH

The purpose of this thesis is to describe the importance and methods used to safely simulate the high-transient, low-duty cycle events that occur within electrical systems. A nondestructive testbed was constructed at NPS to examine the effects of radiated magnetic and electric fields on electrical and electronic components. The testbed injects radiated fields into the EUT using small near-field test probes. One test probe is used to create magnetic fields and the other probe is used to create electric fields. An example circuit board was tested to demonstrate how the EUT responds to the electric and magnetic fields. The goal of the test is to inject electric and magnetic fields using near field test probes and pinpoint the components that are susceptible to electric or magnetic fields coupling. The frequency and amplitude of the radiated fields are controlled by the user. Once the weak points in the system have been identified, the engineers or board designers can use this information to correct the problematic areas and increase its robustness. This improves the overall operational performance of the EUT and ensures the product is robust to unwanted EMI [1], [5], [10].

The basic concept being used was created by Dr. Michael Schutten and has been patented under Patent No: U.S. 6,242,925 B1 on June 5, 2001. The test setup has been modified to incorporate newer equipment and tools. The radiated waveform has high

instantaneous energy and very low average power [5]. Thus, the radiated signal will have large instantaneous field strength and very low duty cycle. This represents the potentially dangerous EMI environment that circuits may be exposed to during transient events in the field [4], [5].

E. THESIS ORGANIZATION

The EMI theory and the different electric and magnetic coupling methods are discussed in Chapter II. The challenges EMI presents on the FLASH project are reviewed in Chapter III. Chapter IV describes the testbed setup and testing procedures. Chapter V covers the test implementation and results. Lastly, Chapter VI outlines the future work that will be conducted for the FLASH project.

II. EMI THEORY

To explain the rationale of this thesis work, some basic EMI theory and concepts are reviewed and explained in this chapter.

A. CAUSES OF EMI

Understanding EMI requires knowledge of magnetic and electric field coupling [4]. Electrical system corruption is caused by the induced currents and voltages that are coupled into the system by the electric or magnetic fields. Specifically, the electric fields induce ground referenced common mode currents and magnetic fields induce differential mode voltages. This externally induced energy can cause interference within a device, circuit, system, or subsystems [1], [4], [13]. A coupling path is required to allow the electric and/or magnetic fields to be received by the system [14]. The diagram shown in Figure 1 describes how energy may be radiated, coupled, received, and then corrupt a circuit [1].

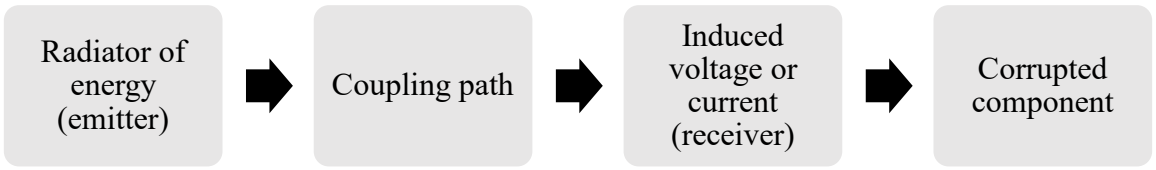

Figure 1. Energy coupling flow path needed to cause EMI

Reduction or removal of any of the steps in the flow path will decrease EMI susceptibility within the system. Therefore, the system designers or testers should focus on individual reduction of each step in the flow path. There are three ways to successfully prevent EMI susceptibility issues as described in Paul (2006):

1. Suppress the emission at its source.
2. Make the coupling path as inefficient as possible.
3. Make the receptor less susceptible to the EMI [induced energy]. [4]

A reliable and efficient way to reduce EMI susceptibility is to limit the emitter as much as possible at the source [4]. To detect possible emitters without constructing the full testbed described in this thesis, an EMC near field test probe can be used to scan the emission source and detect EM induced energy while in normal operating conditions. Once the problematic components/emitters are identified the circuit can be redesigned to reduce or eliminate the unintentional emission of EM energy. There are other ways to fix EMI susceptibility issues as well, and all solutions should be tested to reduce EMI as much as possible during the system design phase [2], [3]. In general, there are four ways to fix EMI issues within an electric circuit or system [1].

1. *Reduce the amount of transmitted or radiated energy from the source (emitter)*. First, try to reduce the size of transmission loops and surfaces present on the circuit board. This can be done by redesigning the board layout to have minimal loop and surface areas on critical circuit regions. Also, try to slow down the rise/fall times within the systems operating frequency. These sharp rise/fall create high dv/dt and di/dt within the system. Often, these solutions are beyond the engineer's or operator's control.

2. *Reduce the coupling path efficiency*. The typical coupling path is often through the air. Therefore, increasing the spacing of the components on the board will reduce the coupling paths strength. This is often not a realistic solution due to the boards predefined size.

3. *Reduce the receiver efficiency*. The goal should be to reduce the receiver loop and surface areas. This will require the board to be redesigned in a more efficient manner, which is very low or no cost, and provides robust, repeatable results.

4. *Reduce or attenuate the incoming high frequency energy*. The three primary ways to attenuate the incoming high frequency are to install shielding, filters, or RF bonding. All three options will be discussed later in this thesis.

The most efficient and cost-effective way to evaluate the system overall EMI susceptibility is to induce electromagnetic energy into the system and measure its resistance to EMI [4], [5]. This method is more effective and practical because it provides a long-term and repeatable solution. The circuit/system is only as strong as the weakest node. To effectively redesign the system, the user must systematically look for the weak or vulnerable points, and then correct them [1], [5]. Therefore, the intention of this thesis is to conduct non-destructive testing to identify the weak point/nodes and use this information to electromagnetically harden the system.

B. COUPLING METHODS

The most common coupling paths for EMI are free space (i.e., air) or electrical traces within the board [15]. The transfer of electromagnetic energy can be broken down into subgroups as defined in MIL-STD 461G [6]. The following bullet list describes the ways electromagnetic energy can be unintentionally transmitted from the emitter to a receiver [4], [6], [16], [17].

- Radiated Emissions (RE) – electromagnetic energy produced by a current or accelerated charge flowing through a wire or conductor [4]. Typically, from an AC power cord [13], [17].
- Radiated Susceptibility (RS) – any component (i.e., antenna) that is susceptible to electromagnetic energy propagating in free space [13], [17].
- Conducted Emissions (CE) – noise current that propagates through AC power cords [16], [17].
- Conducted Susceptibility (CS) – products can be susceptible to a wide variety of interference signals that enter it via the ac power cord. An example is lightning-induced transients [4], [17].

Typically, longer lengths of cables are more efficient at emitting or picking up electromagnetic energy [1], [4], [6], [10]. Therefore, a longer cable or power cord (1m or

more) will act like an "antenna" and pick-up or radiate energy. Radiated energy refers to energy transferred by propagating electromagnetic waves via free space [15]. Conducted energy refers to electromagnetic energy that is transferred on metal surfaces [4], [13]. Usually, conducted waves transfer unintentional electromagnetic energy more efficiently than radiated waves [4], [10], [13].

There are four major coupling methods to induce EMI into a system: magnetic field coupling, electric field coupling, common impedance coupling, and electromagnetic (antenna) coupling [1]. The next sections will describe each coupling path in greater detail.

1. Magnetic Field Coupling

Magnetic field coupling is created by a current flowing in a closed loop conductor in an alternating current (AC) circuit. This magnetic field can potentially be coupled into a system and have adverse or unintended effects on its performance [4], [13]. When a magnetic field is coupled into a circuit it acts like an induced differential mode voltage source, and is fundamentally inductive, represented as $e = M\ {di}/{dt}$, where e is the induced voltage in the receiving loop, M the mutual inductance between the loops, and i the current flowing in the transmitting loop. Thus, it is caused by a time changing magnetic flux and responsible for many EMI problems.

The magnetic flux is coupled between two or more circuits via loops or turns of a wire [4], [13]. For a transformer to maximize magnetic flux transmission, the loops must be physically near each other, have a relatively large loop area, use a high permeability coupling material, and be orientated parallel to one another [1], [4]. These are the same principles that apply to an air core transformer. Therefore, to reduce EMI susceptibility, the designer should try to make a bad air-core transformer [1]. This can be accomplished by reducing the loop areas, increasing the loop spacing, use low permeability coupling materials, or interrupting the magnetic flux coupling [1].

Faraday's Law mathematically explains what is happening between the magnetic field probe and the circuit board. Recall, the time rate of change of magnetic flux linkages that are "cutting the loop" induces a voltage in the closed loop [1].

$$\bar{\nabla} \, x \, \bar{E} = \, - \, {}^{\partial B}/_{\partial t} \quad or \quad \oint_l \; E \cdot dl = \, - \iint_s \; {}^{\partial \mu H}/_{\partial t} \cdot ds \tag{1}$$

In (1), ∇ is the curl of the electric field E, ${}^{\partial B}/_{\partial t}$ represents the time changing magnetic flux. Furthermore, μ is the permeability of the magnetic flux path, for free space it is $4\pi*10^{-7}$ H/m ~ 1 μH/m [1]. The time changing magnetic field intensity is represented by ${}^{\partial \mu H}/_{\partial t}$.

Typically for the purpose of EMI susceptibility testing, the number of "turns in the loop" (*N*) for the product is usually one. The magnetic field injection test probe used in this thesis has a three-turn loop and an area of about 1 in^2. The induced voltage is proportional to the loop area and time derivative of magnetic flux density.

$$V = \, -N \, x \, Area(Loop) \, x \, {}^{\partial \mu H}/_{\partial t} \tag{2}$$

The steady-state excitation voltage *v* that is induced while the system is producing a constant frequency *f* will be calculated while the system is under normal operating conditions [1], [18]. The voltage will become:

$$|v| = N \, x \, 2\pi f \, x \, \mu H \, x \, Area \tag{3}$$

Therefore, for a fixed magnetic field intensity (*H*), as the frequency (*f*) increases, the induced voltage (*v*) will increase proportionally. Engineers can expect to see more board failures at higher frequencies due to this magnetic field coupling mechanism.

2. Electric Field Coupling

Electric field coupling occurs when there is a time changing electric flux ($\partial D/\partial t$) between two surfaces or metal plates, which referred to as a displacement current. The time changing electric flux, ($\partial D/\partial t$) requires an AC signal and it induces an AC conduction current in the circuit. When there is a displacement current, there will also be a conduction current flowing. Displacement current is due to a time changing electric flux, while conduction current is due to moving charges. Conduction current is what engineers refer to when they say a "current is flowing." Displacement current is the principle used in

capacitors to transfer energy between two metal plates or surfaces. The time changing voltage between the metal plates have a displacement current between them. Since the two surfaces are part of a closed loop current path, a conduction current will also exist within the system. This is the basic principle of electric field coupling [1].

Ampere's Law is used to describe how a magnetic field is created by a conduction current (*J*) and a time changing electric flux ($\partial D/\partial t$) across a capacitor.

$$\bar{\nabla} \, x \, \bar{H} = \mathrm{J} + {}^{\partial D}/_{\partial t} \tag{4}$$

The electric flux ($\partial D/\partial t$) will begin on one of the surfaces and terminate on the other. This will be added to the conduction current density (*J*). The two surfaces within the capacitor will develop a displacement current, which creates magnetic fields identical to a conduction current [1], [18]. The resulting displacement current is due to the dv/dt between the two surfaces. This displacement current is part of a closed loop current conduction path, and is the basic concept of electric field coupling.

Electric fields can be electrically coupled into surfaces located within a circuit. If an electric flux is radiated around a circuit board, then this electric flux will develop a displacement current on a circuit board. This displacement current that flows then becomes part of the conduction current path within the closed loop of a circuit. This unintended conduction current may corrupt the intended operation of the circuit, resulting in EMI problems.

3. Common Impedance Coupling

Common impedance coupling requires two or more common electrical connections or circuits carrying currents in a mutual wire. This type of EMI is typically referred to as crosstalk and engineers will often consider the problem as "noise." Figure 2 shows a simple circuit to demonstrate common impedance coupling [1].

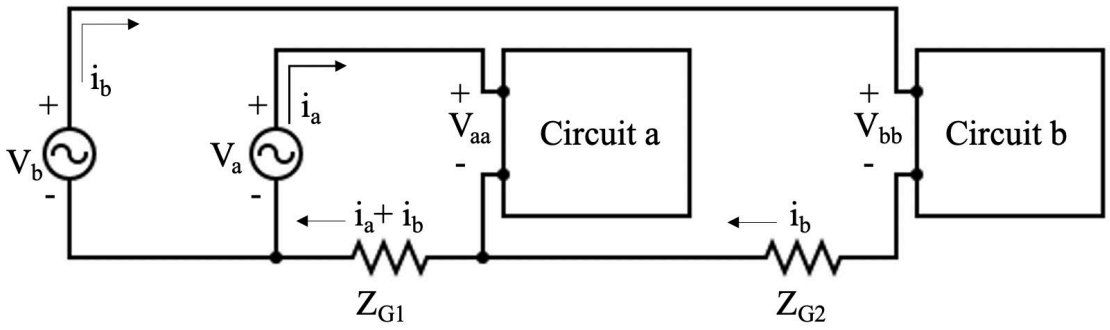

Figure 2. Example circuit of common impedance coupling. Adapted from [1].

The system setup shown in Figure 2 is problematic because the voltage of Circuit a (V_{aa}) is influenced by the current in Circuit b (i_b). The equations below show the voltage seen by Circuit a and Circuit b [1]:

$$V_{aa} = V_a - (i_a + i_b)*Z_{G1} \text{ and } V_{bb} = V_b - (i_a + i_b)*Z_{G1} - i_b*Z_{G2} \quad (5)$$

The voltage of Circuit a is dependent on the current from Circuit b. If Circuit b is a digital circuit and experiences high frequency currents, Circuit a will experience a voltage induced from this current. This is potentially problematic if the engineer does not want Circuit a to interfere with Circuit b. Therefore, circuits should not share a common current conduction path, if possible [1].

4. Electromagnetic Coupling

Antennas are the primary emitter and receiver that use electromagnetic coupling [4], [10], [13]. As electromagnetic waves travel in free space, they can potentially be picked up by circuit boards that have unintentional antennas on them [4]. Traces on circuit boards, or wires in a system, can appear as dipole antennas and are most efficient when greater than 1/4 of the transmitted signal wavelength. For example, a 100 MHz signal will have a wavelength of 3.0 m. Therefore, if the length of the antenna is greater than 3.0/4 = 0.75 m or ~30 inches, the signal can efficiently couple into a system. As frequency increases the wavelength decreases, making electromagnetic coupling problematic at higher frequencies [1], [10].

Electromagnetic coupling may also occur between multiple layers of a printed circuit board (PCB) [1], [13]. The striplines or microstrip lines located within a PCB can act as a transmission line and result in the radiation of EM energy [13]. As seen in [13, p. 395] a stripline consist of a trace symmetrically located between two planes and functions as a transverse electromagnetic (TEM) transmission line. Conversely, Ott states [13, p. 392] a microstrip line consist of a trace above a reference plane and functions as a non-TEM. Longer striplines or microstrip lines (i.e., > 1m) act like antennas while operating at high frequencies (i.e., > 30 MHz) and produce an electromagnetic field that can be coupled into nearby systems [13]. Often, striplines produce a smaller electromagnetic field and result in fewer electromagnetic coupling issues. Due to the complexity of striplines, they are more expensive than microstrip lines.

The most common type of unintentional antennas that can cause a system to have EMI susceptibility issues due to electromagnetic coupling are long wires [4], [13]. This includes power cables that may be energizing the circuit board. Navy ships and aircraft are particularly prone to electromagnetic coupling because of the long cable runs needed to power nearby equipment [10]. There are several regulations for commercial and military applications out lined in "*Manual of Regulations and Procedures for Federal Radio Frequency Management*" [19].

C. PATH OF LOWEST IMPEDANCE

The current that flows in a circuit must return to the source via the path of lowest impedance. EMI issues are typically caused by an unknown or an uncontrolled current return path [1]. As circuit boards are being designed, the engineer must closely track where the currents are flowing and understand why currents flow in that path. Lower frequency signals, typically less than 1 kHz will take the path of lowest resistance. Higher frequency signals, typically greater than 10 kHz, will take the path of lowest inductance, which is typically the smallest loop area. It is important to understand that currents must return to the source and form a closed loop [1]. Understanding where current flows is key to preventing EMI.

D. SHIELDING

Magnetic field shielding needs to be electrically thick to reduce or prevent magnetic field coupling. The thickness of the shielding is measured in skin depths and depends on the frequency of the coupled magnetic field. At higher frequencies the skin depth becomes smaller, and for a fixed thickness increases the overall effectiveness of the shielding [1], [20]. As the shielding thickness increases, the effectiveness also increases. Magnetic field shielding does not require the shield to be grounded or referenced to a defined potential, and the shield acts like a "shorted turn" [21].

For electric field shielding, the shield thickness does not matter, and the shield must be grounded or referenced to a defined potential. The metal shielding needs to be connected to its reference potential (ground) using a relatively shore wire. The length of the wire needs to be much shorter than a wavelength (λ) / 20. The shield can be considered a capacitor plate that is connected to reference potential, or to ground. Therefore, the induced common mode current will be directed away from the system [1].

EMI can be shielded using sheets of metal to make the coupling or receptor path less efficient or susceptible. However, shielding is not always the ideal solution. Shielding can be installed or serviced incorrectly, eliminating its usefulness. Over the life of the product, the shielding may need to be uninstalled and re-installed many times, presenting the possibility of installation errors or shield degradation. Also, shielding is a physical component, so adding shielding adds weight, volume, and cost to any system. This trade-off is not economical or practical for aircraft systems. Larger shielding on cables is also counter-productive for aircraft systems because electrical conductors will need to be larger to account for heat dissipation through the shield.

E. OTHER COMMON ISSUES

Many engineers do not consider the risks of EMI susceptible systems during the initial design of an electrical circuit or system. Once the design is complete and the physical board is tested in the lab, the operator may notice unplanned or unexpected operation. This is the result of poorly designed systems that emit or receive unintended energy, causing the

board or system to not function correctly. Reasons why EMI is difficult for engineers to reduce are as follows: [1], [4]

1. *Parasitic inductances and capacitances*. The parasitic inductance and capacitance do not appear on the circuit schematic, but they often impact the system. Also, the way these impact the system can be counterintuitive and cause confusion.
2. *The current return path is not well controlled while designing the circuit.* This unintentional current flow can induce EMI within multiple parts of the circuit.
3. *Multiple EMI problems can occur at once*. Having more than one problem within a system makes it difficult to identify and uncouple the individual problems (e.g., EMI from magnetic and/or electric field coupling).
4. *Engineers often classify EMI as 'noise" and discount the impact*. This implies that there is no easy solution and noise is simply accepted as byproduct of the electrical circuit physical components.
5. *Most engineers have not had formal training or education on EMI or EMC*. The causes and effects of EMI are not taught in many academic environments, leading to engineers unfamiliar with their signs and symptoms.

F. KEY TAKEAWAYS

Several principles related to signal emission, coupling, and reception were discussed throughout this chapter. Below is a short list of ways to reduce EMI susceptibility of a circuit efficiently and effectively. To reduce EMI susceptibility, the circuit engineer should try to:

- Reduce the amount of transmitted or radiated energy from the source (emitter).
- Reduce the efficiency of the coupling path.

- Reduce the receiver efficiency.
- Reduce or attenuate the incoming high frequency energy.

Furthermore, below is a list of key takeaways that are referenced throughout this thesis.

- Magnetic field coupling is proportional to the transmitting loop current frequency and amplitude. This means the radiated signal will increase proportionally as frequency or amplitude increase.
- Magnetic field injection will appear as a differential mode voltage source induced into the electrical circuit. The circuit loop inductance is important for the equivalent circuit, and is proportional to the square of the number or turns, and the loop area.
- Electric field injection coupling is represented by an induced ground referenced common mode current source augmented into the circuit under test.
- Electromagnetic coupling can be caused by long power cables.
- EMI issues are often caused by an unknown or an uncontrolled current return path. The current that flows through a circuit must return to the source via the path of lowest impedance.
- The effectiveness of magnetic field shielding depends on its thickness and does not need to be referenced or grounded. The effectiveness of electric field shielding does not depend on the shield thickness; however, the shield must be grounded, or referenced to some other defined potential.
- Shielding is often not the best solution for EMI susceptibility issues because it is heavy, costly, and can degrade over time.

THIS PAGE INTENTIONALLY LEFT BLANK

III. CHALLENGES PRESENTED BY EMI WITHIN THE FLASH CIRCUIT BOARD

The solid-state circuit breaker developed in the FLASH project is rated 2 kV and 1.2 kA. During a system fault, the fault current can rise as high as 5 kA. Clearing such high fault currents within tens of microseconds leads to high dv/dt and di/dt and severe EMI issues. To achieve the ambitious high-power density goals of FLASH, the size of the circuit breaker is minimized. Thus, the unintentional coupling between noise sources and loads is made worse, increasing the EMI design challenges. This chapter will focus on the EMI challenges presented by the FLASH circuit board.

A. FLASH SYSTEM SPECIFICATIONS

The circuit diagram for the solid-state circuit breaker is shown in Figure 3.

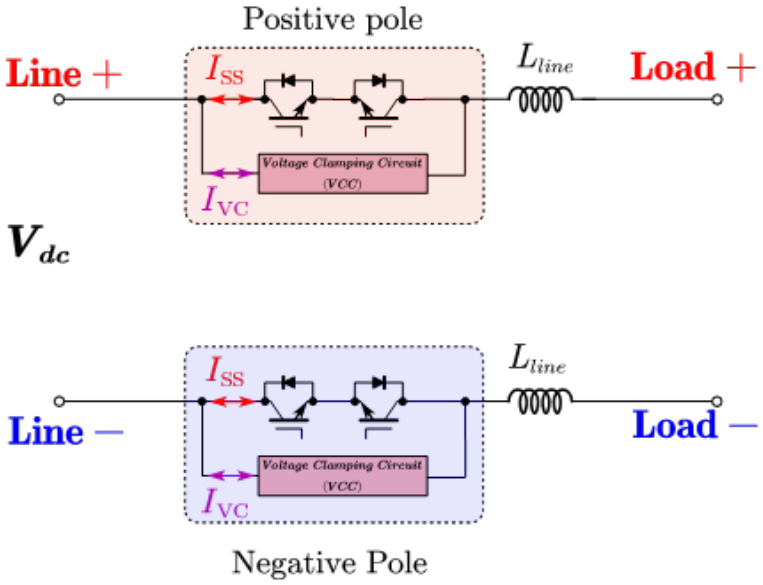

Figure 3. Topology of the solid-state circuit breaker in the FLASH system (image taken from FLASH team)

The unit consists of two identical circuit breakers, one in each dc pole. Each circuit breaker includes two IGBTs with anti-parallel diodes. These two IGBTs are connected

anti-series to block bipolar voltage and carry bidirectional current. A voltage clamping circuit (VCC) is connected across the two IGBTs to absorb energy when clearing the fault current. The key specifications of the system are listed in Table 1.

Table 1. Key specifications of the FLASH solid-state circuit breaker

Rated voltage	+/- 1.0 kV (or 0–2.0 kV)
Rated current	1.2 kA continuously
Response time	10 μs
Maximum fault current	5 kA
Specific power density	>100 kW/kg
Efficiency	99.5%

Figure 4 shows the proposed solid state circuit breaker system. Its mechanical dimension without external busbar is 0.34m×0.38m×0.16m and its weight is about 18 kg. So, the specific power density is about 130 kW/kg and the power density is 116 MW/m^3.

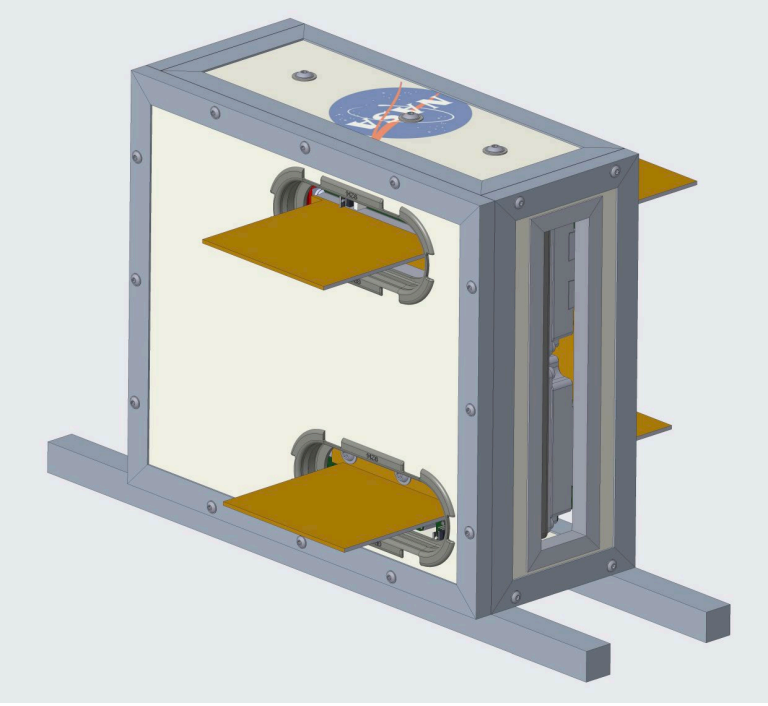

Figure 4. NASA FLASH solid state circuit breaker design (image taken from FLASH team)

The circuit breaker has a metal frame and some metal panels. This provides mechanical support and acts like a partial shield for EMI. However, due to mechanical design and insulation design constraints, this chassis is not a good Faraday cage. Thus, it cannot provide effective shielding from EMI.

The internal structure of the circuit breaker is displayed in Figure 5.

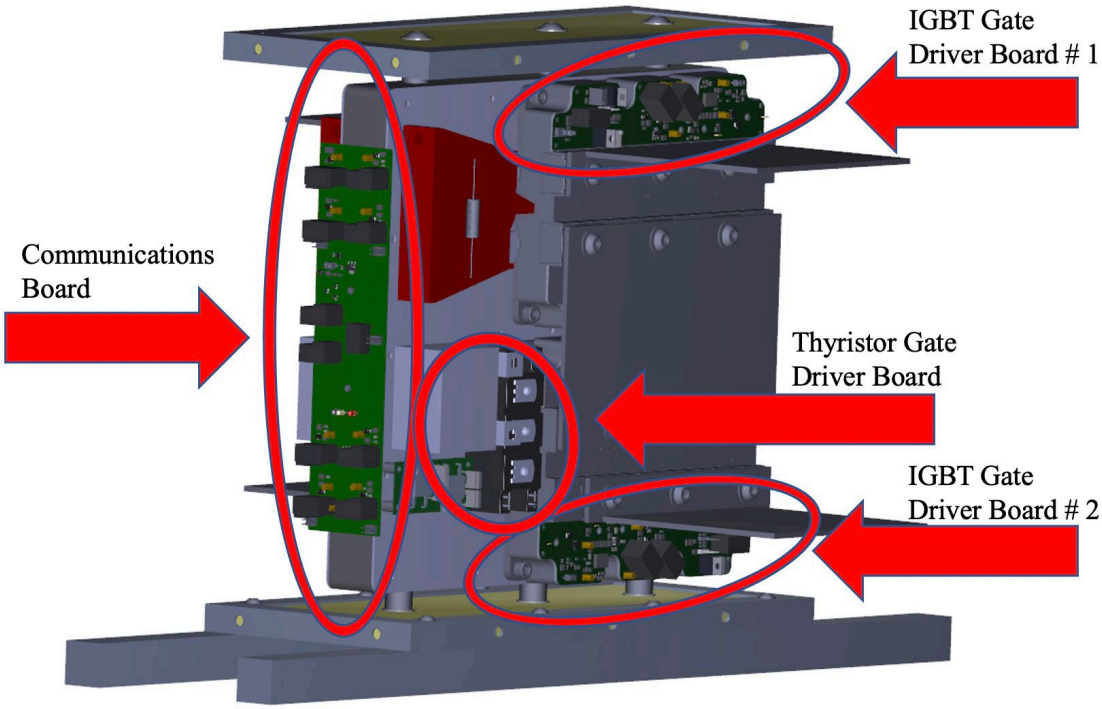

Figure 5. Topology of the proposed circuit breaker (image taken from FLASH team)

For each pole, there are two gate drive circuit boards for the two IGBT modules and one gate drive circuit board for the thyristor module. The two breakers share a digital control board. All the circuit boards are close to the high-power components. For example, the busbar can carry 5 kA, which must be cleared in less than 10 μs and radiates a very strong magnetic field. The communication board is located on the rear of the circuit breaker and mounted vertically. If any of the logic circuit is compromised, it can lead to false trigging of the circuit breaker and permanently damage the power devices. This design

makes the circuit breaker compact, but also limits the amount of shielding that can be used around the logic boards. Therefore, each of the logic boards must be tested for EMI susceptibility, and then redesigned to be more robust in its operating environment.

B. POTENTIAL DESIGN / OPERATING CHALLENGES

The logic boards within the FLASH circuit breaker are exposed to a hostile EMI environment created by the FLASH circuit breaker itself, and other systems on the aircraft. The potential causes of EMI that will impact the FLASH system logic boards are:

- Fast switching within the circuit breaker creates a high dv/dt and the resulting electric flux induces a common mode current to flow internally within the chassis. This common mode current may flow through the logic boards and corrupt their intended operation. For example, a low or "OFF" signal can be unintentionally switched on a high or "ON" signal, causing the logic board to malfunction.

- The common mode current will flow in a closed loop within the circuit breaker. Such common mode currents are generated internally as mentioned above, or externally by other components in the system. However, in either case, the induced currents may be created and then coupled into the nearby logic boards.

- A current with a large di/dt through the negative and positive bus creates a significant magnetic field problem. This magnetic field can couple into the logic boards and induce a voltage into the circuit under test [1]. Recall from Chapter II, magnetic field coupling will induce a differential mode voltage that can affect the intended operation of a logic board.

- The frame is not a Faraday cage. Therefore, the frame may act like an antenna and pick-up EM energy from other sources in the operating environment. Furthermore, other nearby components (not associated with the FLASH circuit breaker) will produce

additional noise which can be coupled into the FLASH logic boards through magnetic field, electric field, or radiation coupling and can corrupt the boards.

The external sources of EMI cannot be controlled. Thus, the effects they have on the FLASH logic boards must be mitigated. Therefore, testing the FLASH logic boards for EMI susceptibility early in the design process is very important. Potentially susceptible components or areas of the boards need to be identified so they can be redesigned to be robust in this harsh EMI environment. The testbed designed in this thesis will identify the weak points on the circuit boards so they can be made more robust and resistant to EMI.

Figure 6 shows how the current flows within the FLASH circuit breaker.

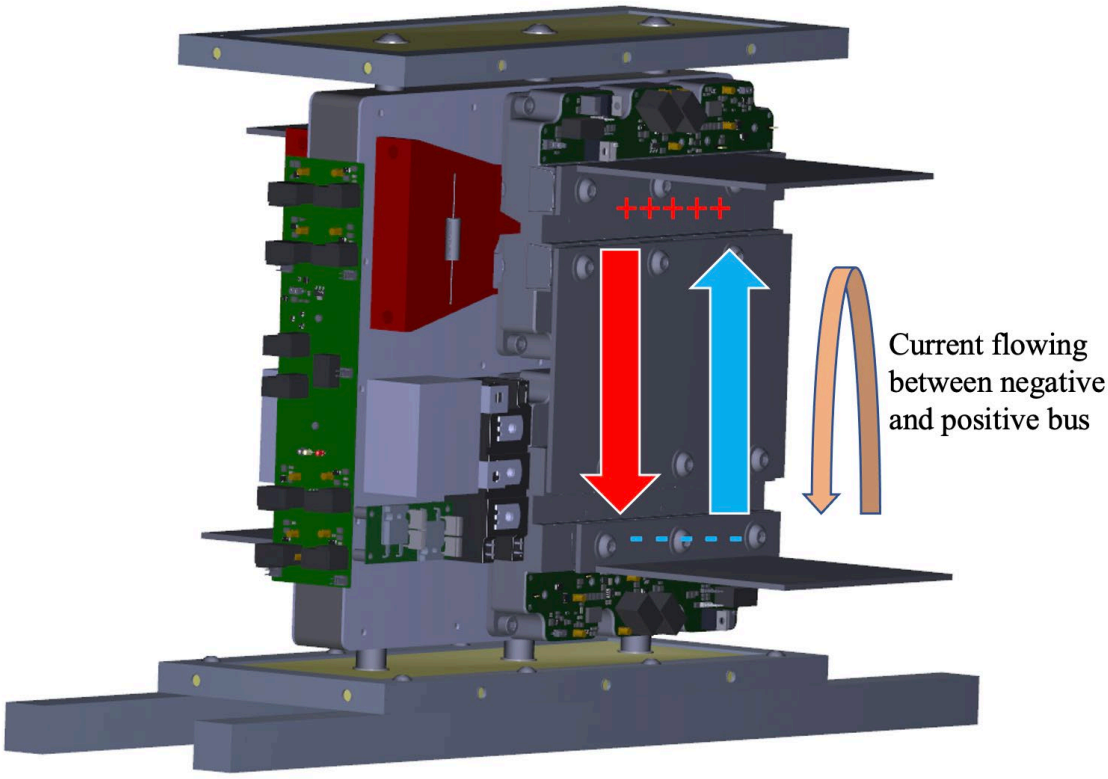

Figure 6. Current paths within the FLASH circuit breaker (image taken from FLASH team)

As the current flows between the positive and negative buses as shown in Figure 6, a magnetic field is produced. The logic boards are located near the path of current flow. Due to the close proximity of the gate driver boards to the generated magnetic field, these logic boards will be especially susceptible to EMI through magnetic and electric field coupling. Again, this is where many of the internal challenges or risks related to EMI susceptibility will occur.

IV. TESTBED DEVELOPMENT

Previous EMI susceptibility testing required large amount of energy to be coupled into systems until the point of failure [5]. This method was often destructive to the EUT and did not identify which specific component was susceptible to EMI within the system [22]. Often, the EUT would be destroyed by the large amounts of induced energy before useful data could be collected. Also, this type of testing is very costly and often does not provide useful information after the test has concluded [22]. One method used to conduct EMI susceptibility testing is called bulk current injection (BCI), it requires the user to inject high frequency currents into a wire harness [23]. This method also tests the system as a whole, but does not identify the individual components that are susceptible. Further, BCI can damage the EUT [5], [23].

The testbed and the related test procedures described in this thesis are significant because they are nondestructive and can pinpoint the individual components susceptible to EMI. Therefore, the EUT can be repeatedly tested, and the results can be quickly quantified. Compared to traditional EMI susceptibility testing, the near field injection discussed in this thesis is more time and cost effective [22], [23].

A. TESTBED SETUP

The procedures used for the proposed testbed are crucial to conducting nondestructive EMI susceptibility testing. The method described in this section will outline how the different pieces of equipment are connected. This section lists the make/model of the equipment used for running the proposed tests.

1. How to Connect the Testbed Equipment

The following is a description of the equipment and the procedure used to replicate an EMI environment that the FLASH circuit breaker and any logic board may experience throughout its operating life cycle. The system shown in Figure 7 is used to couple magnetic and electric fields into the circuit boards to test their EMI susceptibility.

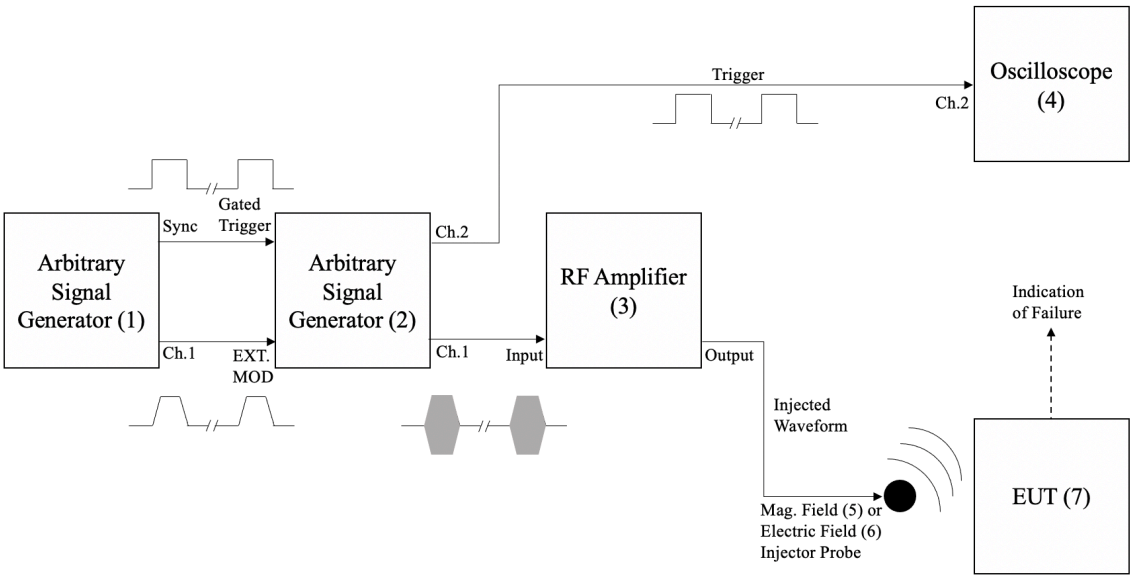

Figure 7. Drawing of testbed setup

Figure 7 shows how the equipment is connected. The numbers (#) on each piece of equipment are used as a reference. The list below outlines the components used to construct the testing platform needed to inject magnetic and electric fields.

1. *Arbitrary signal generator* (1) – Generates the trapezoidal envelope signal for the electric or magnetic field waveform with a low (e.g., 1%) duty cycle. The amplitude and frequency of this waveform is controlled from the front of the signal generator. Adjusting the amplitude determines the slope of the trapezoidal waveform. Adjusting the frequency will determine how many of these trapezoidal waveforms are generated per second. The sync channel is connected to the other arbitrary signal generator (2), this signal is used as a gated trigger. The reason why a trigger is needed will be discussed below in section B.

2. *Arbitrary signal generator* (2) – This component has two purposes. First, create a sinusoidal waveform that is modulated by the trapezoidal signal from Channel 1. Second, to create a gated trigger from the sync signal via Channel 2. Channel 1 Output: The trapezoidal signal outline from (1) connects to the I/O modulation external input of (2). A controllable

sinewave is modulated with the trapezoidal signal to create the waveform shown in the next section of this chapter. The resulting waveform is connected to the RF amplifier (3) using a BNC cable. The amplitude and frequency of the sinewave are controlled by the dial on the front of the arbitrary signal generator (2). Channel 2 Output: The sync signal from (1) connects to the external input of (2) and then used to create a gated trigger. This new gating signal is sent into Channel 2 of the Oscilloscope (4). The purpose of this gated trigger will be discussed in later in section B of this chapter.

3. *RF power amplifier* (3) – The amplifier is used to increase the RF signal power generated by the arbitrary signal generator (2). This ensures the signal sent to the magnetic and electric field injector probes is large enough to impact the EUT.

4. *Oscilloscope* (4) – Connected to the trigger line of the arbitrary signal generator (2) via Channel 2. Channel 1 Purpose: Depending upon the equipment being tested, Channel 1 may or may not be connected to the EUT. For example, when injecting energy into an IGBT gate drive board, we may monitor the gates emitter voltage with the oscilloscope. Then we would ensure the gate source does not improperly turn on or off in the presence of injected magnetic or electric fields, as the probes are moved or scanned over the EUT. Channel 2 Purpose: A trigger is set on Channel 2 to ensure the oscilloscope is only displaying/updating when RF energy is injected into the system.

5. *Magnetic field injector probe* (5) – This probe is connected to the RF Power Amplifier output using a BNC cable that injects a single frequency, localized, high-frequency near-field magnetic field into the EUT. The injected magnetic field will induce a differential mode voltage source into the EUT.

6. *Electric field injector probe* (6) – This probe is connected to the RF Power Amplifier output using a BNC cable that injects a single frequency, localized, high-frequency near-field electric field into the EUT. Recall, the injected electric field will induce a common mode current source into the EUT.

7. *Equipment Under Test* (EUT) (7) – The circuit board or system being tested for EMI susceptibility.

8. *Oscilloscope Probe* (8) – Used to connect to Channel 1 of the Oscilloscope (4) to the EUT.

9. *Near Field EMC Test Probe Set* (9) – It is used to verify the injector magnetic and electric fields and it is connected to Channel 1 of the oscilloscope (4).

A photo of the completed testbed used in this thesis is shown in Figure 8.

Figure 8. Photograph of the testbed as set up in the laboratory

Figure 8 illustrates the size and of the equipment used in Figure 7. The equipment is intentionally setup to show the sequential flow of the testbed so the reader can understand how each the piece of equipment is connected.

2. Testbed Operation

The testbed shown in Figure 7 and Figure 8 is used to create a nondestructive EMI environment that is needed to test components for EMI susceptibility using radiated magnetic and electric fields. The radiated fields will be generated using two arbitrary signal generators and then sent to the radio frequency (RF) power amplifier. The modulated RF signal is then coupled into different points of the circuit board (i.e., EUT) using near field injector probes. The user can then scan the EUT with the near field injector probes to determine the points vulnerable to EMI via magnetic or electric field coupling. The near field injector probes can be moved to different points throughout the EUT to ensure each subsystem or component within the circuit board is tested individually. Also, the user can increase the signal frequency and amplitude to verify the EUT operation over a wide range of operating conditions. The EUT may or may not be connected to an oscilloscope to display when a nondestructive EUT failure occurs [5].

The purpose of this procedure is to systematically test the EUT for potential EMI susceptibility issues. As discussed in Chapter II, the magnetic field injector probe will radiate a near field magnetic field that can be coupled into the EUT via loops on the board. Magnetic field coupling will induce a differential mode voltage into the EUT and can be strong enough to corrupt the boards intended operation. Also, the electric field injector probe will radiate a near field electric field that can be coupled into the EUT via metal surfaces on the board. Electric field coupling will induce a ground referenced common mode current to flow in the closed loop of the EUT. This induced current can corrupt the EUT normal operating conditions or logic signal.

3. Detailed Description of the Equipment used in the Testbed

Table 2 lists the manufacturer and model number for equipment used in the testbed.

Table 2. Description of equipment used in the testbed

Component Number	Component Name	Equipment Manufacture	Model Number	Specifications	Figure Reference Number
(1)	Arbitrary signal generator	Agilent	33220A	BW: 20 MHz	Figure 9
(2)	Arbitrary signal generator	Rigol	DG5252	BW: 250 MHz	Figure 10
(3)	RF power amplifier	Amplifier Research (AR)	50A250	Power: 50 W BW: 250 MHz	Figure 11
(4)	Oscilloscope	Tektronix	DPO 2012	BW: 100 MHz	Figure 12
(5)	Magnetic field injector probe	Schutten Technical Consulting	N/A	Area: 1 in^2	Figure 13
(6)	Electric field injector probe	Schutten Technical Consulting	N/A	Size: 0.75 in. x 0.75 in.	Figure 14
(7)	Equipment Under Test (EUT)	N/A	N/A	N/A	N/A
(8)	Oscilloscope probe	One end BNC and other test clips	N/A	200 MHz 10 M Ω/<10pF 10X	Figure 15
(9)	Near Field EMC Test Probe Set	Tekbox	TBPS01	H-Field and E-Field	Figure 16

The arbitrary signal generator (1) used to create the outline of the trapezoidal waveform is shown in Figure 9. The output signal is going to the modulation input, and the sync signal is going to the gated pulse input on the other arbitrary signal generator (2).

Figure 9. Photograph of the arbitrary signal generator (1)

The arbitrary signal generator (2) is used to create the sinewave that is modulated with the trapezoidal waveform, and is shown in Figure 10. This signal generator also creates the gated pulse trigger that is sent to the oscilloscope (4). A key feature of this signal generator is that it allows the user to vary the frequency and amplitude of the sinewave with the dial on the front of the machine.

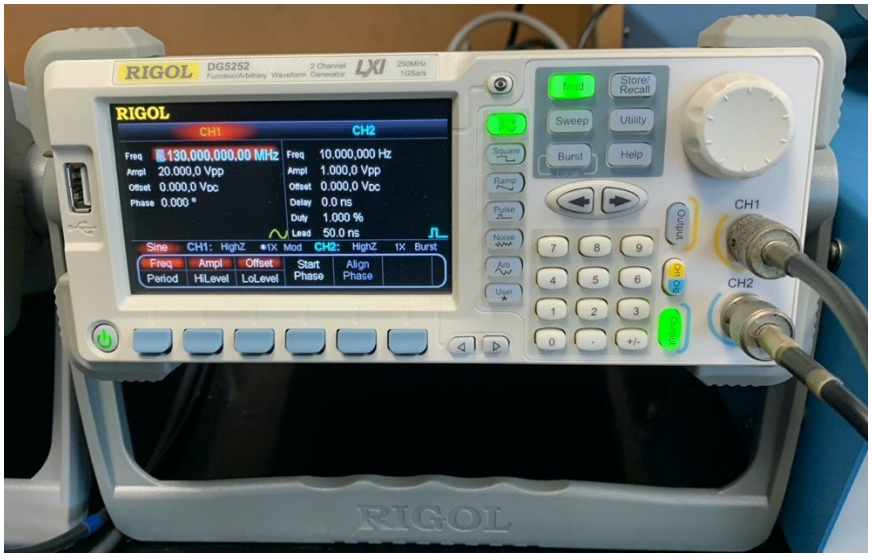

Figure 10. Photograph of the arbitrary signal generator (2)

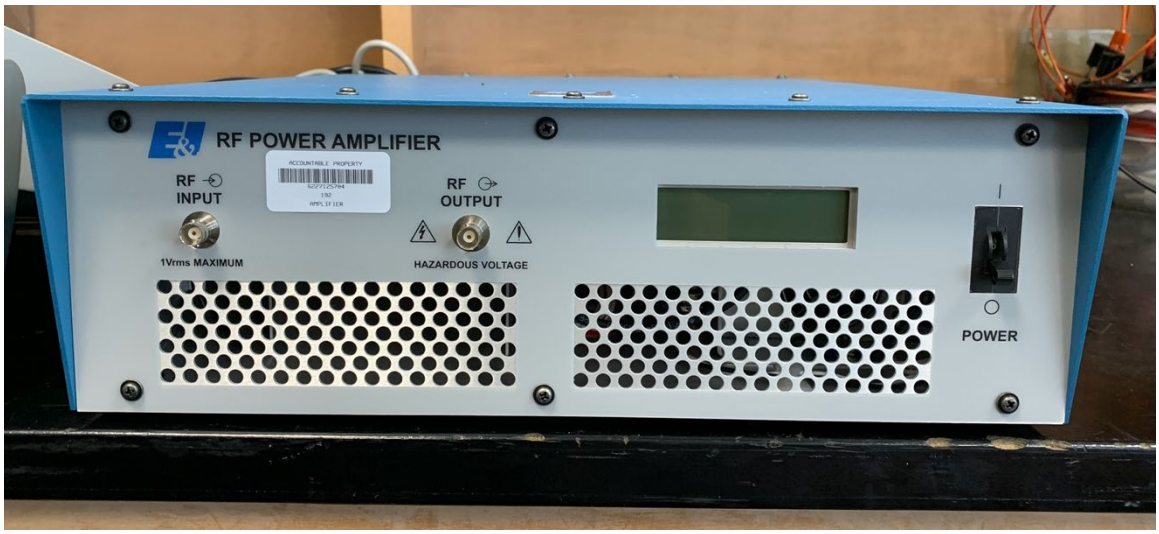

Figure 11. Photograph of RF power amplifier (3)

The RF power amplifier (3) shown in Figure 11 is used for the testing conducted in this thesis. However, using a RF power amplifier with a higher bandwidth (greater than 250 MHz) is recommended to ensure all potentially hazardous frequencies are tested. The RF power amplifier listed in Table 2 is recommended for further testing.

The oscilloscope (4) is used to view the systems response shown in Figure 12. Notice the oscilloscope is gated using the trigger signal into Channel 2.

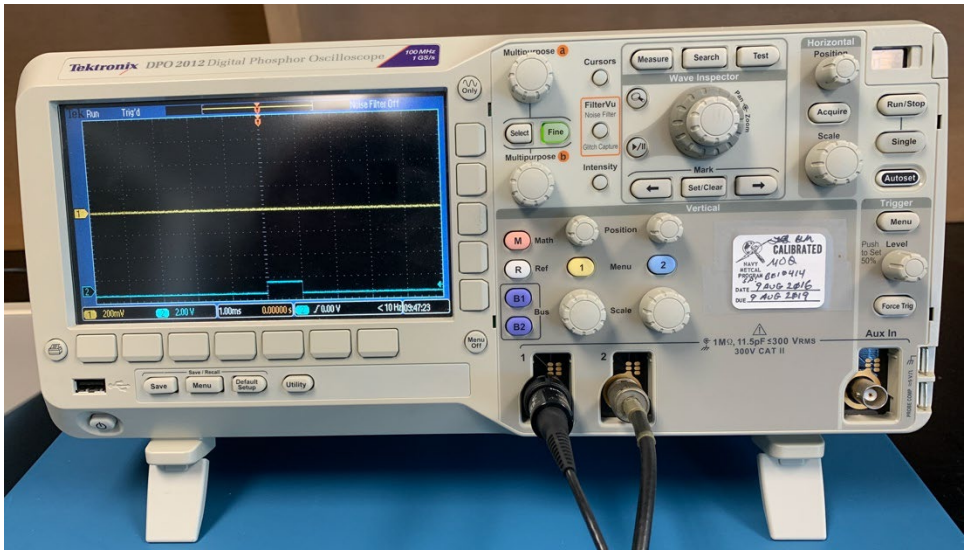

Figure 12. Photograph of the oscilloscope (4)

The test procedures discussed in this thesis describe how the magnetic field injector probe is acting like half of an air core transformer due to the loop on the near field probe and the radiated magnetic flux. The other half of the air core transformer is a loop on the circuit board that may be susceptible to the radiated energy being coupled into it. Therefore, the testing apparatus is recreating a hostile electromagnetic environment. The magnetic field probe is one half of the transformer, and the board is acting as the other half. Figure 13 shows photographs of the magnetic field injector probe used to emit a magnetic field onto the EUT.

Figure 13. Photograph of top and bottom view of the magnetic field injector probe

The magnetic field injector probe shown in Figure 13 is constructed using a BNC connector consisting of a three-turn loop of wire. This three-turn loop is Faraday shielded using a copper screen. The loop area of the magnetic field injector probe is approximately 1 in^2. A high voltage Nomex insulator is glued to the probe.

In this thesis, an electric field injector probe is used to act as a capacitor plate. The electric field injector probe has a metal plate that emits an electric field and can couple into different surface areas of the EUT. Circuit boards often have surfaces areas that act like the other half of the capacitor, where the electric field couples into the system. Once the electric field is coupled, the induced current will flow in a closed loop within the EUT and may be strong enough to corrupt the EUT intended operation. The electric field probe is emulating

large transient events that can happen while the system is operating. As electric field coupling occurs, the equivalent circuit is a common mode current source that is ground referenced. The strength of the common mode current source will depend on the amount of energy being radiated by the electric field probe. Figure 14 shows a photograph of the electric field probe used in this thesis.

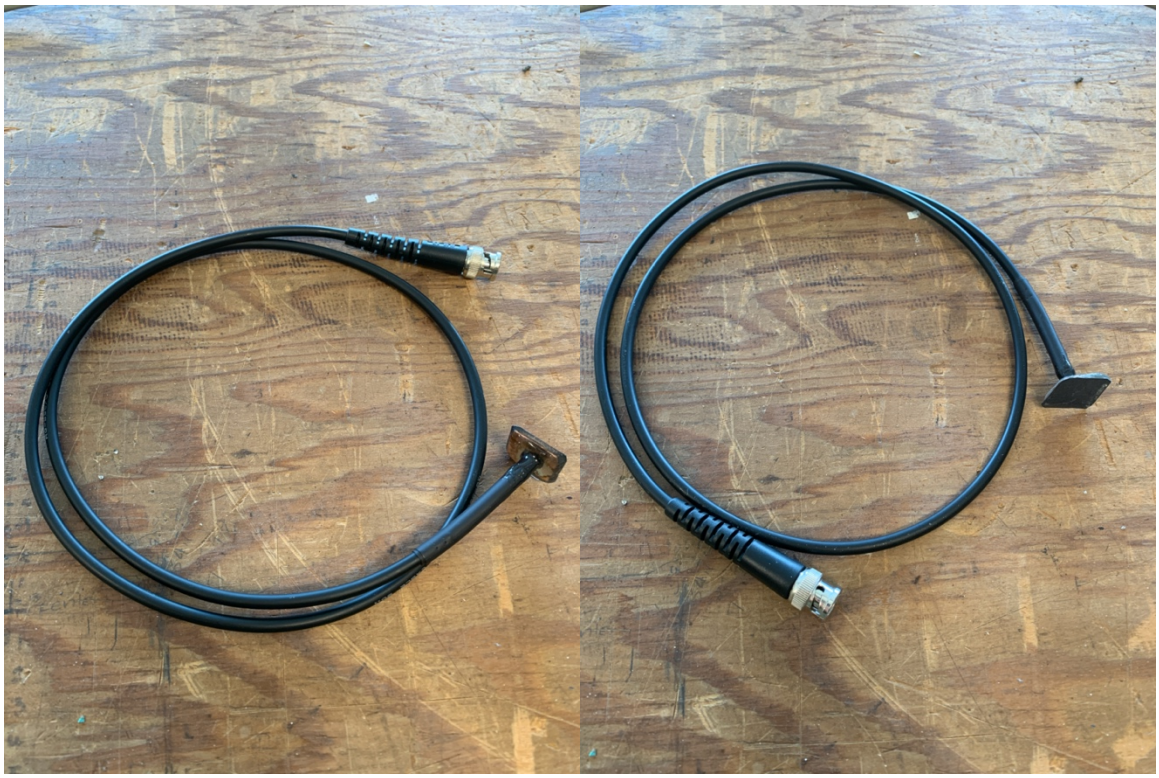

Figure 14. Photograph of the top and bottom view of electric field injector probe

The electric field injector probe has a BNC connector on one end and the metal surface on the other. The electric field injector probe is approximately 0.75-inches by 0.75-inches. A Nomex insulator is bonded to the metal surface of the probe.

Figure 15. Photograph of oscillograph probe (8)

The oscilloscope probe (8) shown in Figure 15 is connected to the oscilloscope (4) and EUT for the test conducted throughout this thesis. However, connecting the EUT to an oscilloscope to observe resulting voltage is not always necessary. For example, EUT that have local displays or indications lights that can alert the user of an error. The oscilloscope (4) and oscilloscope probe (8) are only required if the EUT does not have an indication of failure or other means of notifying the tester when a failure occurs.

Figure 16. Photograph of the near field EMC test probes (9)

The near field EMC test probe set is used to verify the operation of the magnetic and electric field injector probes. The near field EMC test probe with the largest loop area is used to verify the operation of the magnetic field injector probe (5) via magnetic field coupling. The near field, electric field EMC sniffer probe is used to verify the operation of the electric field injector probe (6).

B. WAVEFORM GENERATION

This thesis describes the importance of performing nondestructive EMI susceptibility testing on electronic circuits and to identify weak points or components on the board that are susceptible to either magnetic or electric field coupled EMI. This test method ensures the test is nondestructive and only a single frequency is injected during each scanning cycle. This allows EMI weak points to be found and corrected leading to more robust operation during its life cycle. This specific type of waveform is needed

because it ensures the EUT will not be destroyed, and only a single frequency is being injected while conducting EMI susceptibility testing.

1. Method Used to Create Injected Waveform

The simulated waveform is designed to emulate the high transient events that a circuit board may experience during its normal life cycle. Only one frequency at a time is injected into the EUT. The waveform needs to have high instantaneous energy and low average power [5]. This is accomplished by creating a waveform with a very high field strength and a very low duty cycle. To generate this specific type of signal, a sinusoidal waveform is modulated with a trapezoidal wave. This produces the described operating characteristics of an EMI environment and recreates events the system will experience during unusually high transients. The shape of this waveform will ensure only a single frequency is injected at a time. The arbitrary signal generator (1) is used to create the trapezoidal wave shown in Figure 17.

Figure 17. Trapezoidal waveform outline (zoomed view)

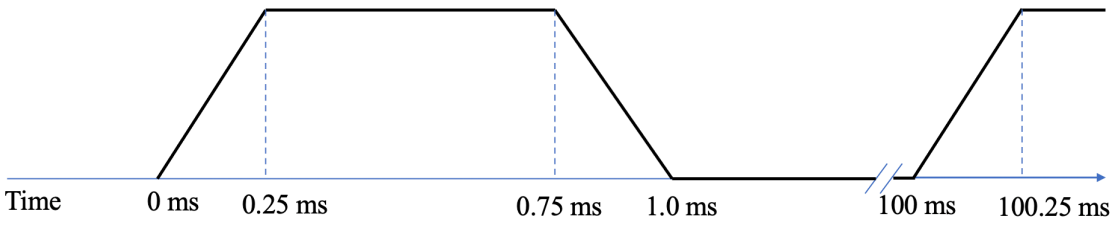

Figure 18. Trapezoidal waveform outline showing long time off

The trapezoidal waveforms shown in Figure 17 and Figure 18 are created by the arbitrary signal generator (1) by setting the operating frequency to 10 Hz and then mapping out the other points manually. Selecting 10 Hz as the operating frequency will result in a time "ON" period of 1 ms, meaning the system will be radiating the waveform for 1ms and off for 99 ms (i.e., duty cycle =1%). The location of each point is show in Table 3:

Table 3. Trapezoidal waveform point map

Point Number	Time (ms)	Voltage (Vpk)
1	0.0 (start)	0.0
2	0.25	1.0
3	0.75	1.0
4	1.0	0.0
5	100 (end)	0.0

From Table 3 and Figure 18, the waveform is "ON" for 1 ms out of its 100 ms period. Thus, the near field injector probes will be injecting ten pulses per second. One of the main reasons for the low duty cycle is to ensure the test is nondestructive and the EUT cannot be damaged due to the high amounts of power being coupled into it. The duty cycle and frequency of the modulated waveform can be controlled by changing the frequency on the arbitrary signal generator (1) or remapping the points.

The next step is to modulate the sinusoidal waveform with the controllable trapezoid. The arbitrary waveform generator (1) sends the trapezoidal waveform outline to the arbitrary waveform generator (2), which generates a sinewave and then amplitude modulates this sinusoidal waveform with the trapezoid. The two waveforms are multiplied together, resulting in a sinewave with a maximum amplitude equal to the trapezoidal outline. Figure 19 shows the resulting AM modulated signal.

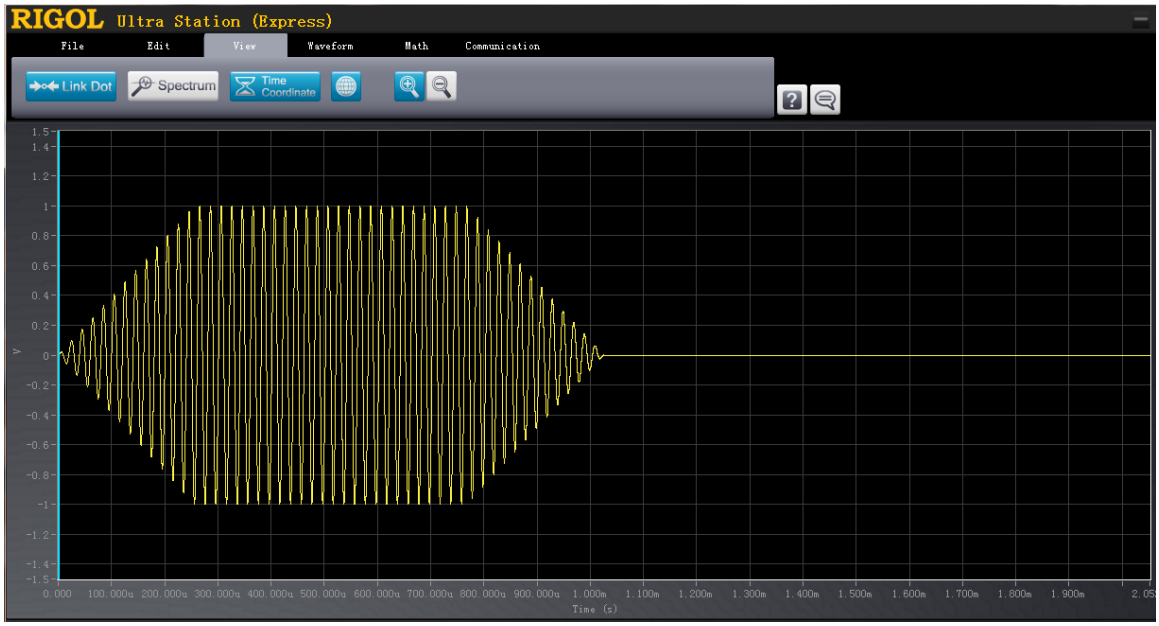

Figure 19. Simulated modulated waveform

Figure 19 shows the result of amplitude modulating the trapezoidal outline with operating frequency of 10 Hz and amplitude 1 Vpk, and a sinewave with operating frequency of 50 kHz and amplitude of 1 Vpk. The frequency and amplitude of the sinewave is controlled by the arbitrary signal generator (2). As the amplitude is changed, the slope of the trapezoid will increase or decrease. This results in a larger or smaller sinusoidal signals having higher or lower dv/dt or di/dt.

The next step includes creating a gated trigger and sending it to the oscilloscope (4). The purpose of the gated trigger is to force the oscilloscope to only show the time periods in which the modulated waveform is being injected. Since the duty cycle is small,

a gated trigger will ensure the oscilloscope is only displaying information when the signal is “ON” and not display the long time periods between pulses. The process of connecting the equipment to generate the gated trigger is also shown in Figure 7.

To begin setting up a gated trigger signal, we connect the sync output from the arbitrary signal generator (1) to the external trigger input on the arbitrary signal generator (2). Next, we program the arbitrary signal generator (2) to use the external trigger input as a reference for a gated pulse signal. Then send the gated pulse from arbitrary signal generator (2) Channel 2 output to the oscilloscope (4) Channel 2 via a BNC cable. Then we configure the oscilloscope (4) to trigger on the gating pulse, which will be concurrent with the trapezoidal waveform outline created on the arbitrary signal generator (1). Again, the purpose of the trigger signal from the arbitrary signal generator (2) is to force the oscilloscope (4) to only display information when the modulated waveform is being injected into the EUT.

2. Method Used to Verify the Injected Waveform

To begin verifying the injected waveform, the testbed is set up in accordance with the description from Chapter IV, section A. Then the magnetic field probe is connected to the RF amplifier (3) and an EMC sniffer test probe (9) is plugged into Channel 1 of the oscilloscope (4). Then we slowly bring the two probes together and watch the voltage on the oscilloscope (4). We observe the amplitude of the voltage increase as the probes get closer to one another. Next, while the probes are touching, we slowly increase the frequency of the sinewave using the arbitrary signal generator (2) and view the injected waveforms modulated frequency and amplitude increase on the oscilloscope (4). Figure 20 shows how to place the magnetic field injector probe (5) and EMC test probe (9).

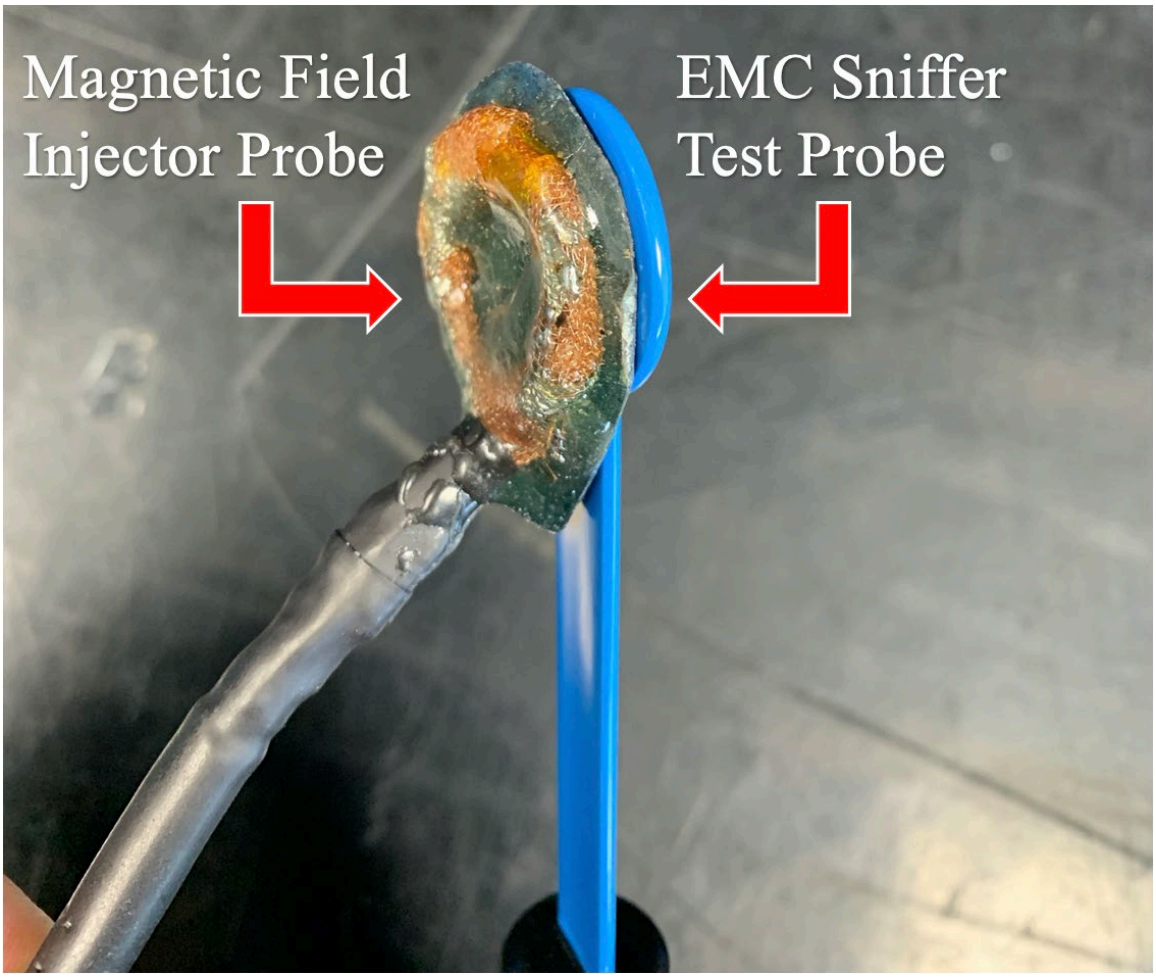

Figure 20. Photograph showing how to connect or touch the magnetic field injector probe (5) and the EMC sniffer test probe (9)

As discussed in Chapter II, while conducting magnetic field injection, the amplitude of the measured waveform will be proportional to the input amplitude and frequency. In other words, doubling the sinewave input amplitude will double the output waveform amplitude. Likewise, doubling the input sinewave frequency will double the output waveform amplitude at this doubled frequency. This is verified in Figure 21 through Figure 23.

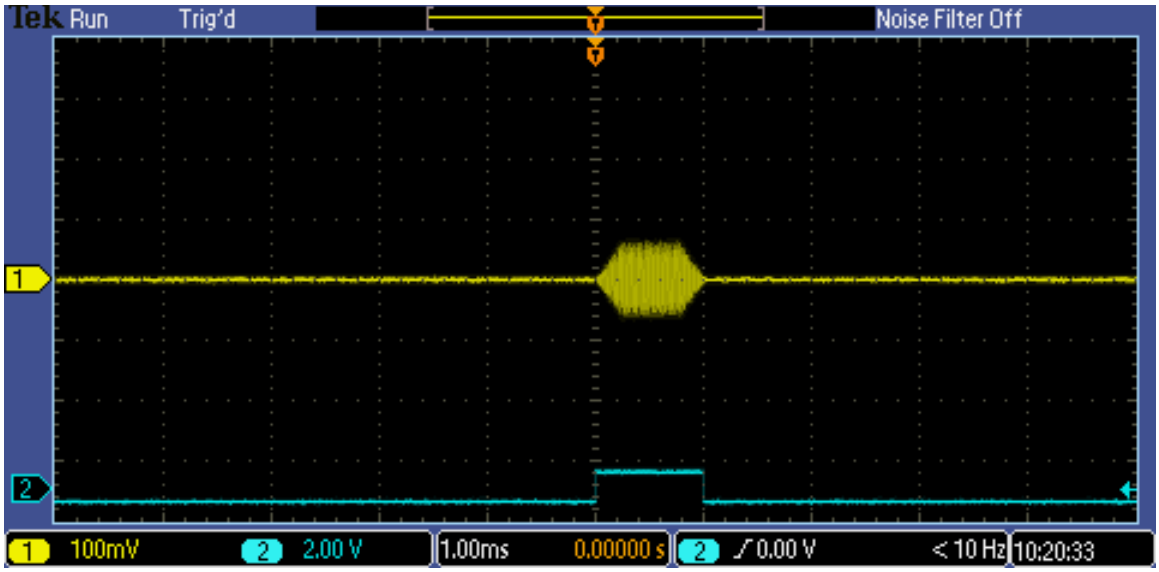

Figure 21. Magnetic field injection verification with input sinewave amplitude = 5.0 Vpk and frequency = 10.0 MHz

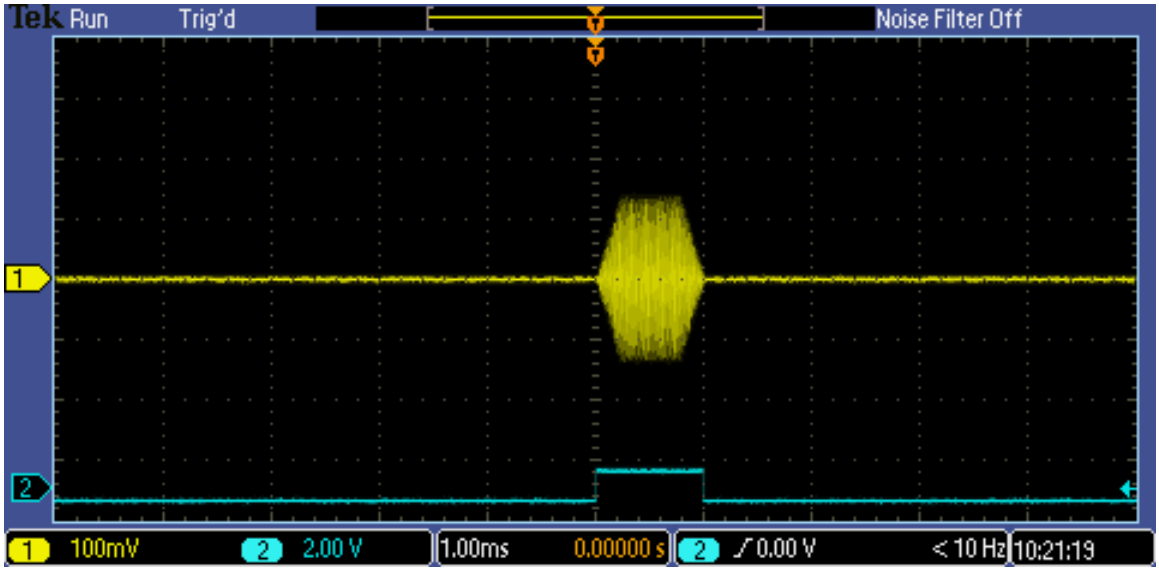

Figure 22. Magnetic field injection verification with input sinewave amplitude = 5.0 Vpk and frequency = 20.0 MHz

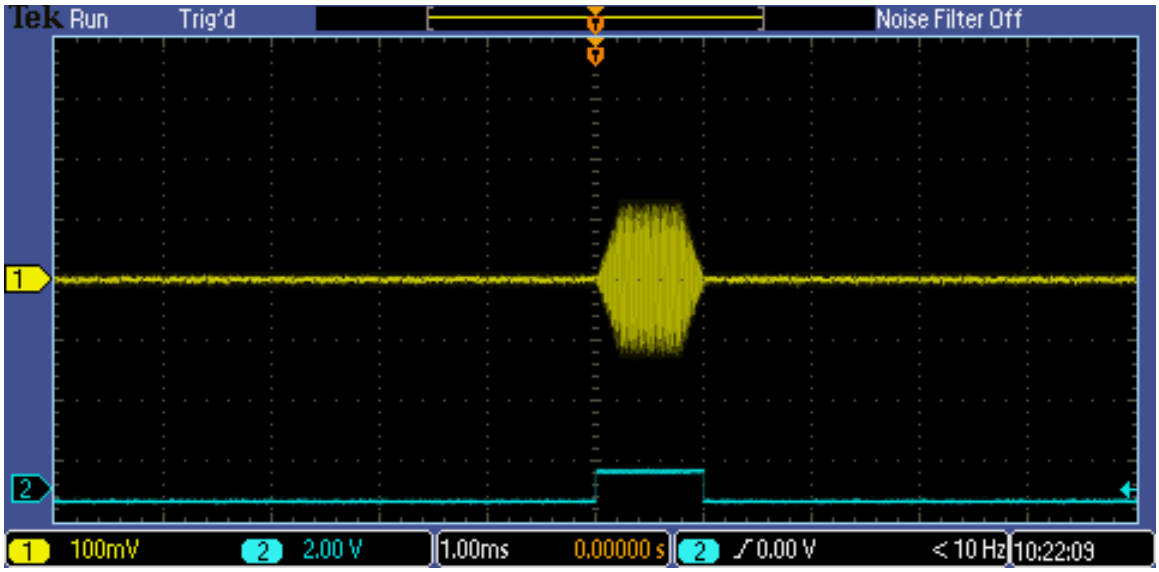

Figure 23. Magnetic field injection verification with input sinewave amplitude = 10.0 Vpk and frequency = 10.0 MHz

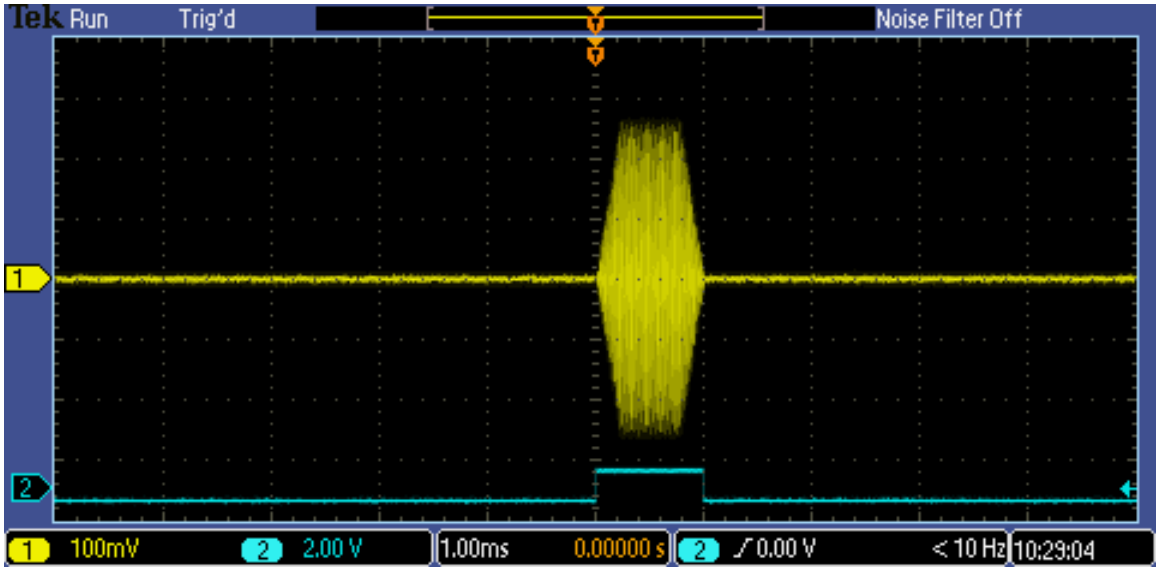

Figure 24. Magnetic field injection verification with input sinewave amplitude = 10.0 Vpk and frequency = 20.0 MHz

Notice in the figures above that doubling the input amplitude of the sinewave resulted in a proportional increase in the measured modulated waveform amplitude. Also, doubling the sinewave input frequency resulted in a proportional increase in the measured modulated waveform amplitude. Lastly, doubling both the amplitude and frequency on the

input sinewave at the same time resulted in a 4x increase of the measured waveform amplitude. Table 4 summarizes the experimental results shown in the figures.

Table 4. Magnetic field injection verification summary

	Input Sinewave Amplitude (Vpk)	Input Sinewave Frequency (MHz)	Resulting Measured Modulated Waveform Amplitude (mVpk)
Figure 21	5.0	10.0	65.0
Figure 22	5.0	20.0	130.0
Figure 23	10.0	10.0	130.0
Figure 24	10.0	20.0	260.0

As shown in Table 4, increasing the input frequency has a proportional impact on the measured waveform amplitude. Doubling both the input frequency and amplitude results in an 4x increase for the measured waveform at the doubled frequency. We have now verified a key principle of magnetic field injection discussed within thesis: changing the input sinewave frequency or amplitude will result in a proportional change in the measured modulated waveform frequency and amplitude.

Next, we verify the measured modulated signal radiated from the electric field injector probe (6) with the near field sniffer probe (9). To do this, we begin by removing the magnetic field injector probe (5) from the output of the RF amplifier (3), and then connect the electric field injector probe (6). Then we slowly bring the two probes together until they physically touch. Figure 25 shows how we connect or touch the electric field injector probe (6) to the near field sniffer probe (9).

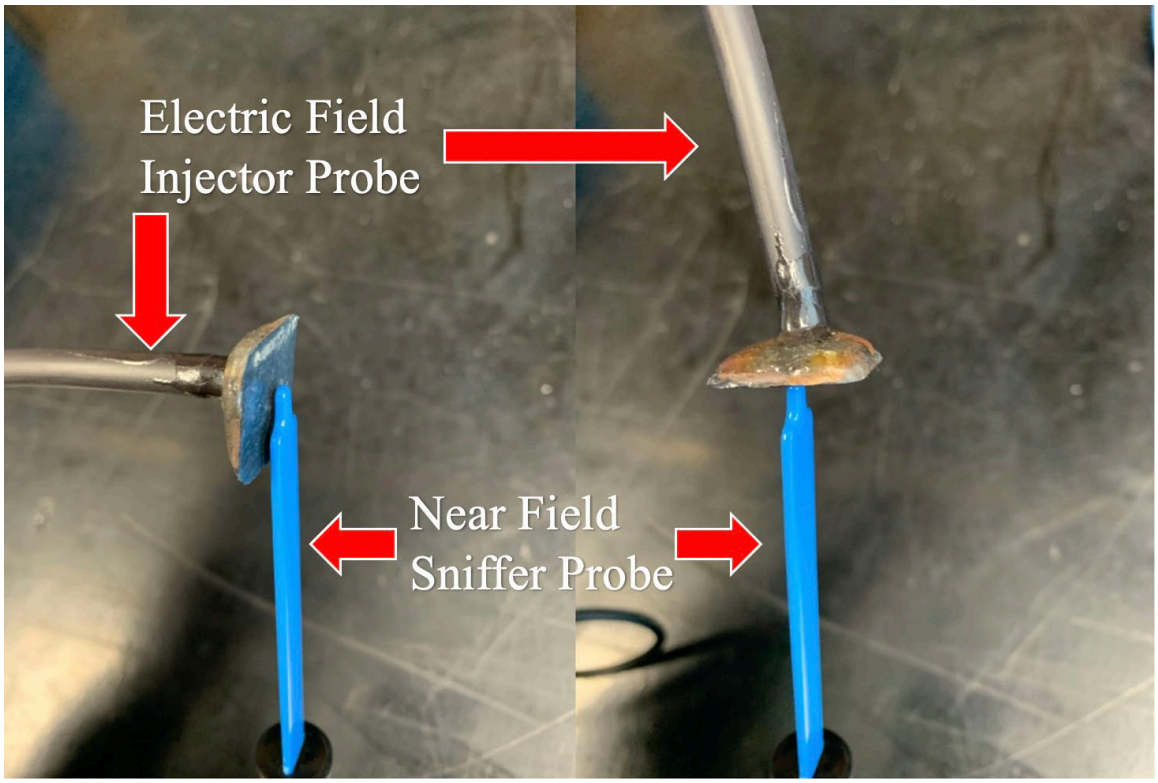

Figure 25. Photograph showing how to connect or touch the electric field injector probe (6) and near field sniffer probe (9)

Notice the placement of the electric field injector probe (6) and the near field sniffer probe (9). The two probes can be positioned at this 90° angle or 180° angle. Similarly, to the verification test of the magnetic field injector probe (5), the shape of the trapezoidal waveform changes proportionally as amplitude and frequency increase or decrease. As discussed in Chapter II, the amplitude of the trapezoidal waveform is proportional to the input frequency and amplitude. Therefore, doubling the input sinewave frequency or amplitude will result in a proportional increase of the measured waveform amplitude. Figure 26 through Figure 29 show the results of the different frequency and amplitude combinations used to verify the electric field injector probe (6) operation.

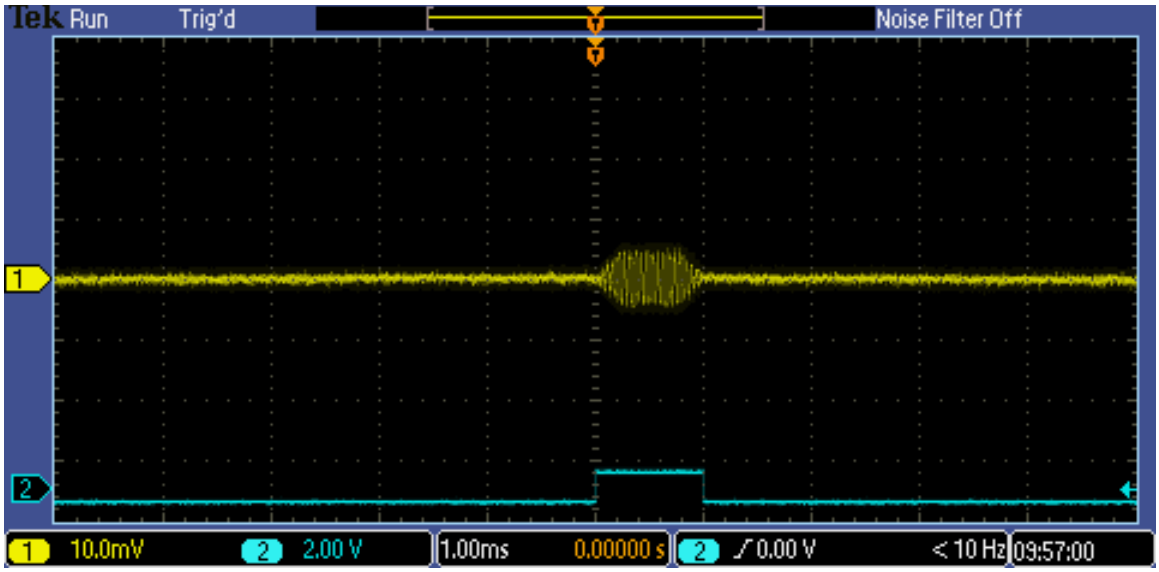

Figure 26. Electric field injection verification with input sinewave amplitude = 5.0 Vpk and frequency = 15.0 MHz

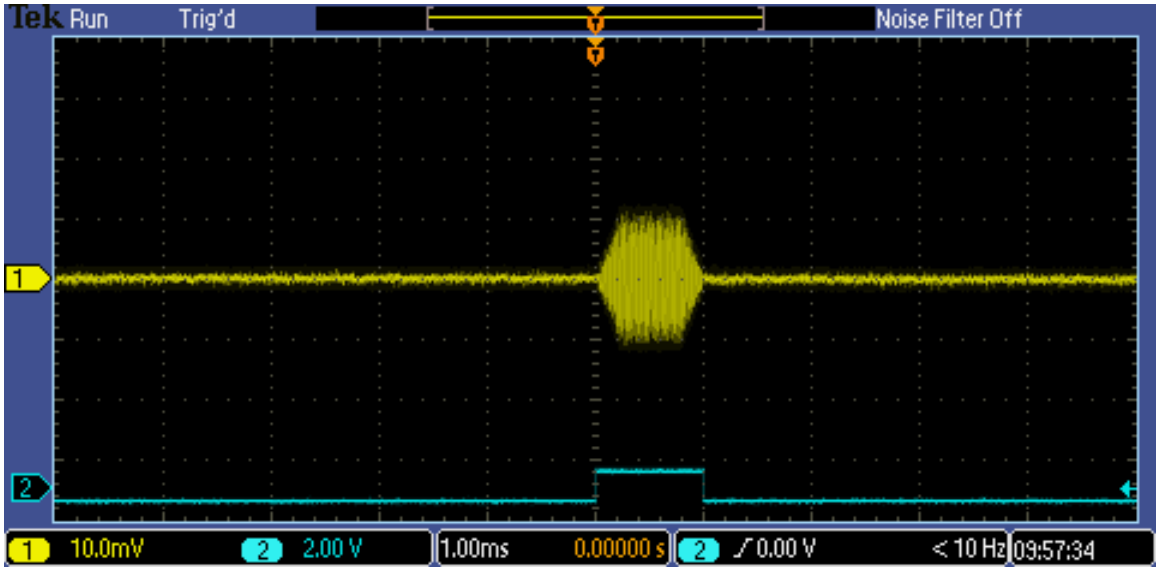

Figure 27. Electric filed injection verification with input sinewave amplitude = 5.0 Vpk and frequency = 30.0 MHz

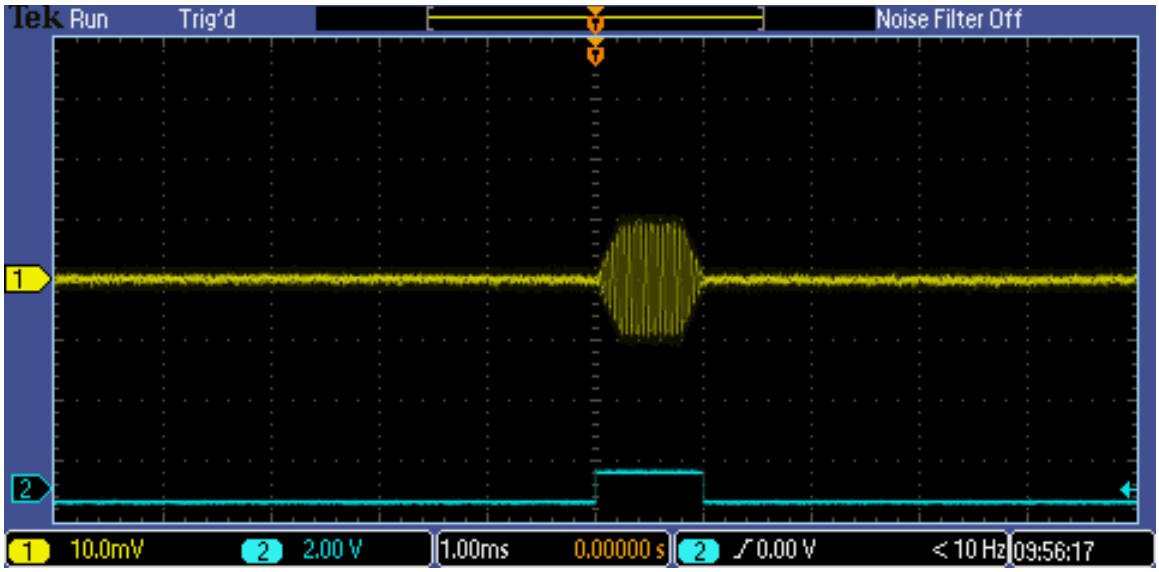

Figure 28. Electric field injection verification with input sinewave amplitude = 10.0 Vpk and frequency = 15.0 MHz

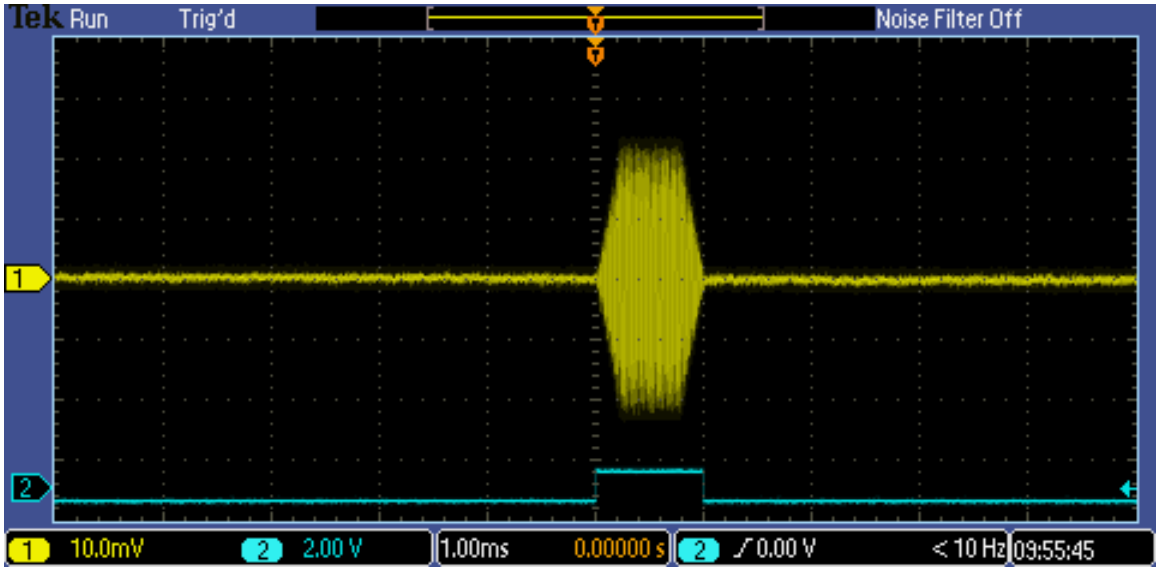

Figure 29. Electric field injection verification with input sinewave amplitude = 10.0 Vpk and frequency = 30.0 MHz

In Figure 26 and Figure 27, doubling the input sinewave frequency results in a doubling of the measured waveform amplitude. Also, in Figure 26 and Figure 28, notice how doubling the input sinewave amplitude resulted in doubling the measured waveform amplitude. Lastly, doubling both the input sinewave amplitude and frequency at the same

time resulted in a 4x larger signal, shown in Figure 29. A summary of the electric field verification test is presented in Table 5.

Table 5. Electric field verification summary

	Input Sinewave Amplitude (Vpk)	Input Sinewave Frequency (MHz)	Resulting Measured Modulated Waveform Amplitude (mVpk)
Figure 26	5.0	15.0	5.0
Figure 27	5.0	30.0	10.0
Figure 28	10.0	15.0	10.0
Figure 29	10.0	30.0	20.0

The results shown in Table 5 verify the theory presented in Chapter II of this thesis. The amplitude of the modulated trapezoidal waveform is directly proportional to both input sinewave frequency and amplitude changes. High-frequency and/or high-power systems will emit large amounts of energy that can be coupled into a nearby system through electric field coupling.

V. TEST IMPLEMENTATION AND RESULTS

The purpose of this thesis is to develop a nondestructive EMI susceptibility testbed used for testing circuit boards in harsh EMI environments. Therefore, an example circuit board with known performance under different electric and magnetic fields is used for proof-of-concept testing. The FLASH system is one example where the tests described in this thesis are applicable. The example circuit board used in this chapter is closely related to the logic circuit boards used in the FLASH system. This proves the theory and operation of all components described within this thesis, and the application can be applied to any circuit boards.

A. HOW TO IMPLEMENT THE TESTBED

Before conducting any EMI susceptibility test, we first verify the output of each near field injector probe, as discussed in Chapter IV, section B. This ensures the testbed is generating the correct waveform and the test can be controlled by the user.

The test is completed using only one near field probe at a time. This process is repeated several times for each near field probe, changing the signal generators frequency or amplitude between sweeps of the entire system. The recommended method we use to sweep the board is detailed in the following steps:

1. Connect one near field injector probe to RF amplifier (3) output.
2. Verify the signal on the oscilloscope per Chapter IV, section B of this thesis.
3. Monitor the EUT for any resulting nondestructive failures.
4. Set the arbitrary signal generator to produce a voltage 0.5 Vpp in amplitude with frequency greater than 0.1 MHz.
5. Slowly scan the board with the near field injector probe and watch the oscilloscope screen for changes in the EUT voltage output.

6. Systematically increase either the frequency or the amplitude of the source voltage produced by the arbitrary signal generator (2). Then repeat Step 5.

7. Continue to systematically increase either the input sinewave frequency or amplitude until all frequency and amplitude ranges are tested.

8. Document any areas of the board that show susceptibility problems. This will indicate areas of the EUT that are susceptible to EMI from magnetic or electric field couplings.

The near field injection tests can be conducted over a range of frequency and amplitudes which should be determined based on additional system analysis. For example, the frequency range can be between 0.1 MHz and 200 MHz. In this thesis, the tests are conducted between 0.1 MHz and 30 MHz. The bandwidth is increased in incremental steps to ensure the entire bandwidth is thoroughly tested. For example, we start the test at 0.1 MHz and then we increase the frequency by a fixed ratio (e.g., 5%) after each sweep. The amplitude is also increased.

B. MAGNETIC FIELD INJECTION TEST RESULTS

For this thesis, an example circuit board is provided by Schutten Technical Consulting LLC and is used as the EUT to prove the theory and procedures presented. A photograph of the printed circuit board is shown in Figure 30 and its electrical circuit is shown in Figure 31. This circuit board is used to verify both the magnetic and electric field principles discussed in this thesis.

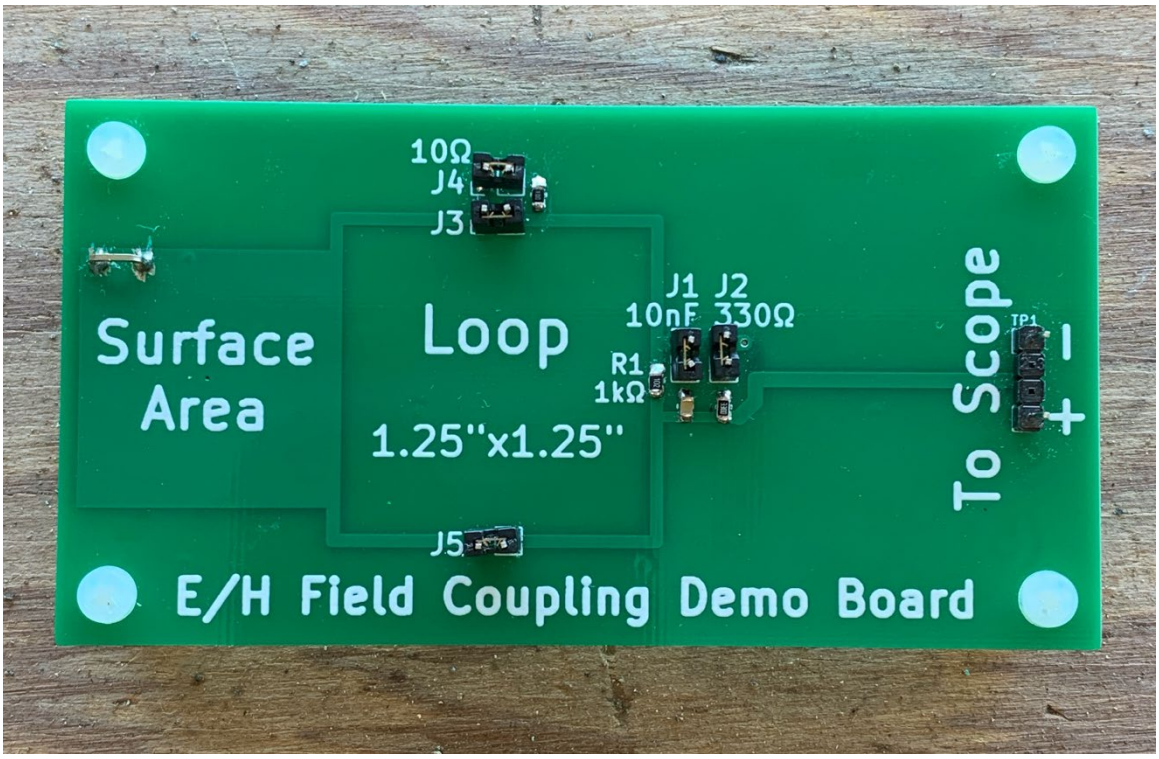

Note: The example circuit board shown in Figure 30 was provided by Schutten Technical Consulting LLC, (518) 847–8334.

Figure 30. Photo of the example circuit board* used as the EUT

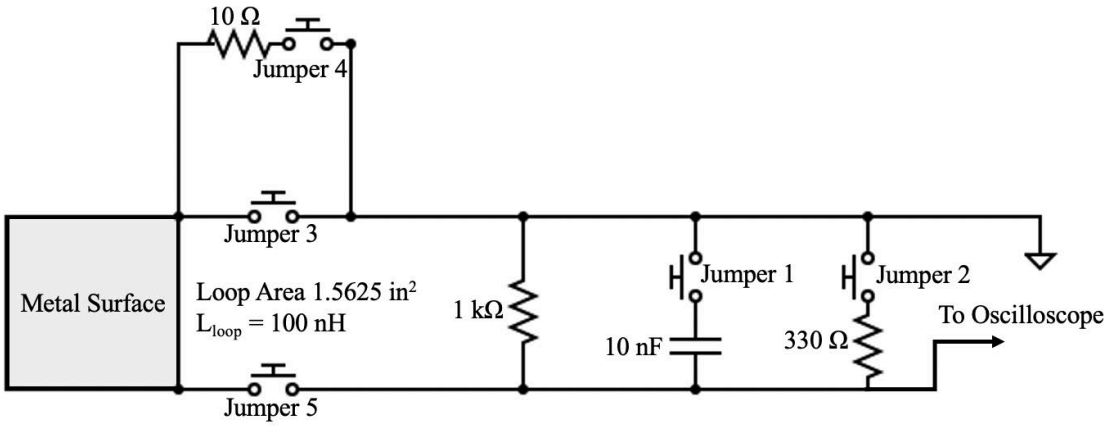

Figure 31. Electrical drawing of example circuit board

As the magnetic field injector probe is applied to the “Loop” shown in Figure 31, the radiated magnetic field is coupled into the example circuit board. This induces a differential mode voltage into the circuit. Also, the 1.25-inch by 1.25-inch single turn

square loop has a parasitic inductance of about 100 nH. Figure 32 shows how the magnetic field injector probe should be coupled into the “Loop” area on the example circuit board while testing. The equivalent circuit resulting from the magnetic field probe injector is applied to the “Loop” area, as seen in Figure 33.

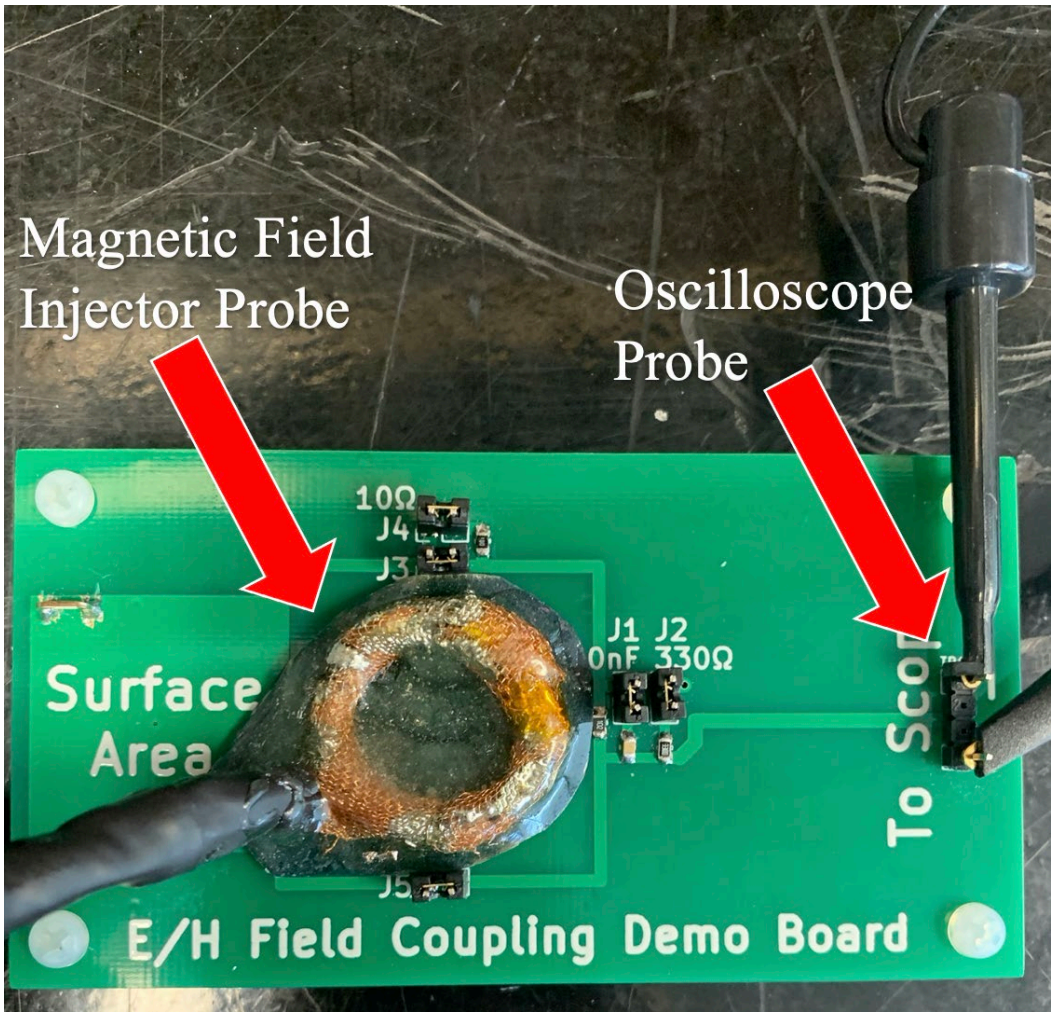

Figure 32. Photograph showing how to apply the magnetic field injector probe to the “Loop” area on the example circuit board

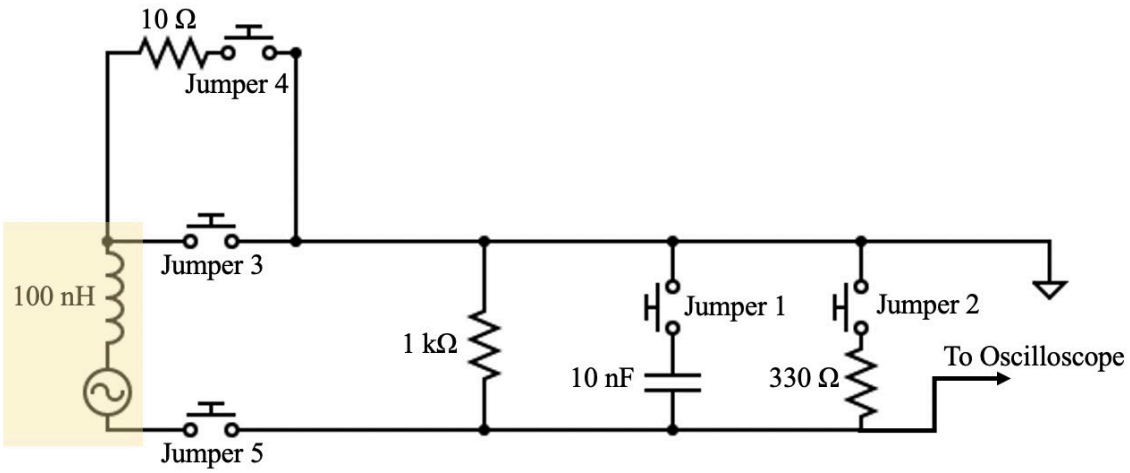

Figure 33. Equivalent circuit drawing of example circuit board while the magnetic field injector probe is applied to the loop area

Figure 33 shows the equivalent circuit that results from coupling the magnetic field probe to the area labeled as "Loop" on the test circuit board. The original circuit is augmented with a differential mode voltage source, and the loop inductance. The amplitude and frequency of the radiated waveform are represented as the AC source in the bottom left corner of Figure 33. The LTspice simulations use the drawing shown in Figure 33 to verify the magnetic field injector test results. Figure 34 shows the equivalent circuit drawing used to simulate the effects of magnetic field injection.

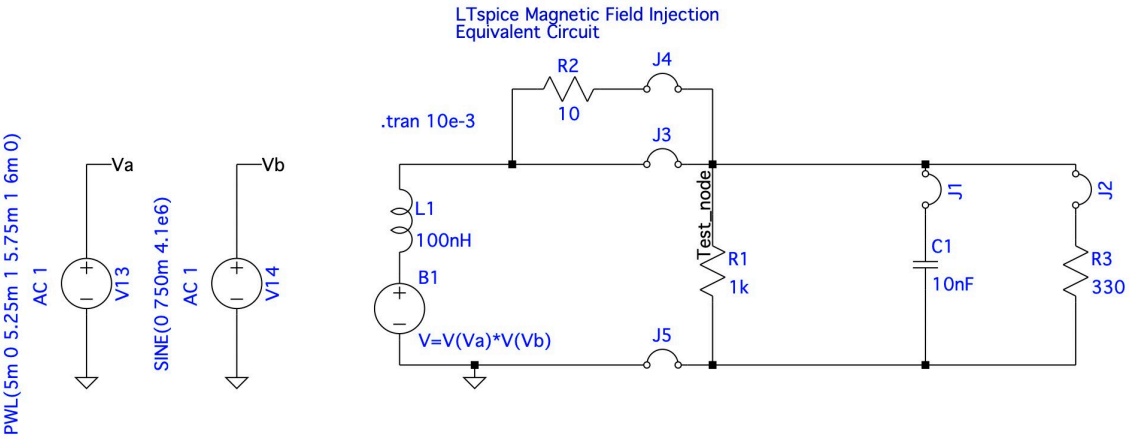

Figure 34. LTspice magnetic field injection equivalent drawing

To begin testing, we connect the example circuit boards to the oscilloscope (4) using an oscilloscope probe (8), as shown in Figure 32. The sequence used to test the circuit boards is done with different jumper combinations. The results and testing configurations are shown in Table 6. The "x" under the jumper column indicates when the jumper is connected to the circuit board. The experimental results were verified with LTspice simulations with the same operating frequency and the same input voltage that was measured using the EMC test probe. Table 6 includes the simulated results as well as the experimental measurements.

Table 6. Results for magnetic field injection testing at frequency = 2.124 MHz and amplitude = 1.0 Vpk

Operating Conditions	Jumper Configuration:					Results:		
Magnetic Field Freq: 2.124 MHz Amp: 1.0 Vpk	J1	J2	J3	J4	J5	Measured Results (mVpk)	Reference Figure Number	LTspice Results (mVpk)
	EMC test probe					1000	Figure 35	N/A
				x	x	750	Figure 36	720
			x		x	780		730
			x	x	x	780		730
No path		x			x	0		N/A
		x		x	x	800	Figure 37	700
		x	x		x	800		730
		x	x	x	x	800		730
No path	x				x	0		N/A
	x			x	x	450	Figure 38	460
	x		x		x	800	Figure 39	900
	x		x	x	x	800		900
No path	x	x			x	0		N/A
	x	x		x	x	450	Figure 40	460
	x	x	x		x	800	Figure 41	900
	x	x	x	x	x	800		900
Ground Reference	x	x	x	x	x	800	No Change	900

The results in Table 6 show the measurements with the magnetic field injector probe radiated on the example circuit board, and also the LTspice simulation results. Again, the input voltage for LTspice was the same as the voltage measured using the magnetic field injector and the EMC test probe to ensure consistent results. The oscillographs of the different operating conditions are shown in Figure 35 through Figure 41. Notice in Table 6 the excellent agreement between the magnetic field injector probe radiated on the test board and the LTspice simulations.

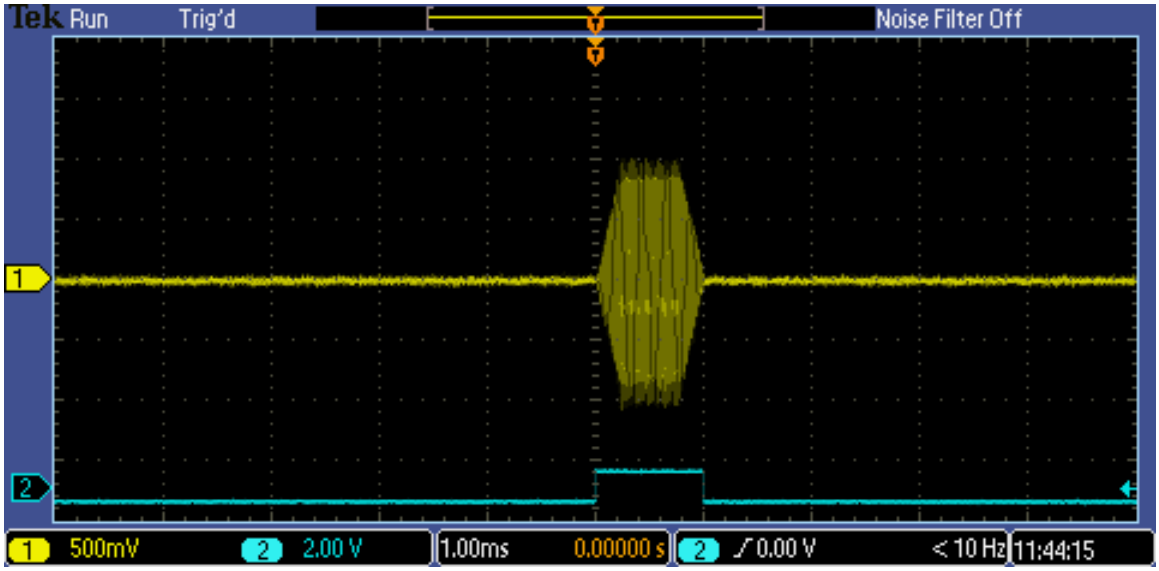

Figure 35. Magnetic field injection - oscillograph of test probe verification

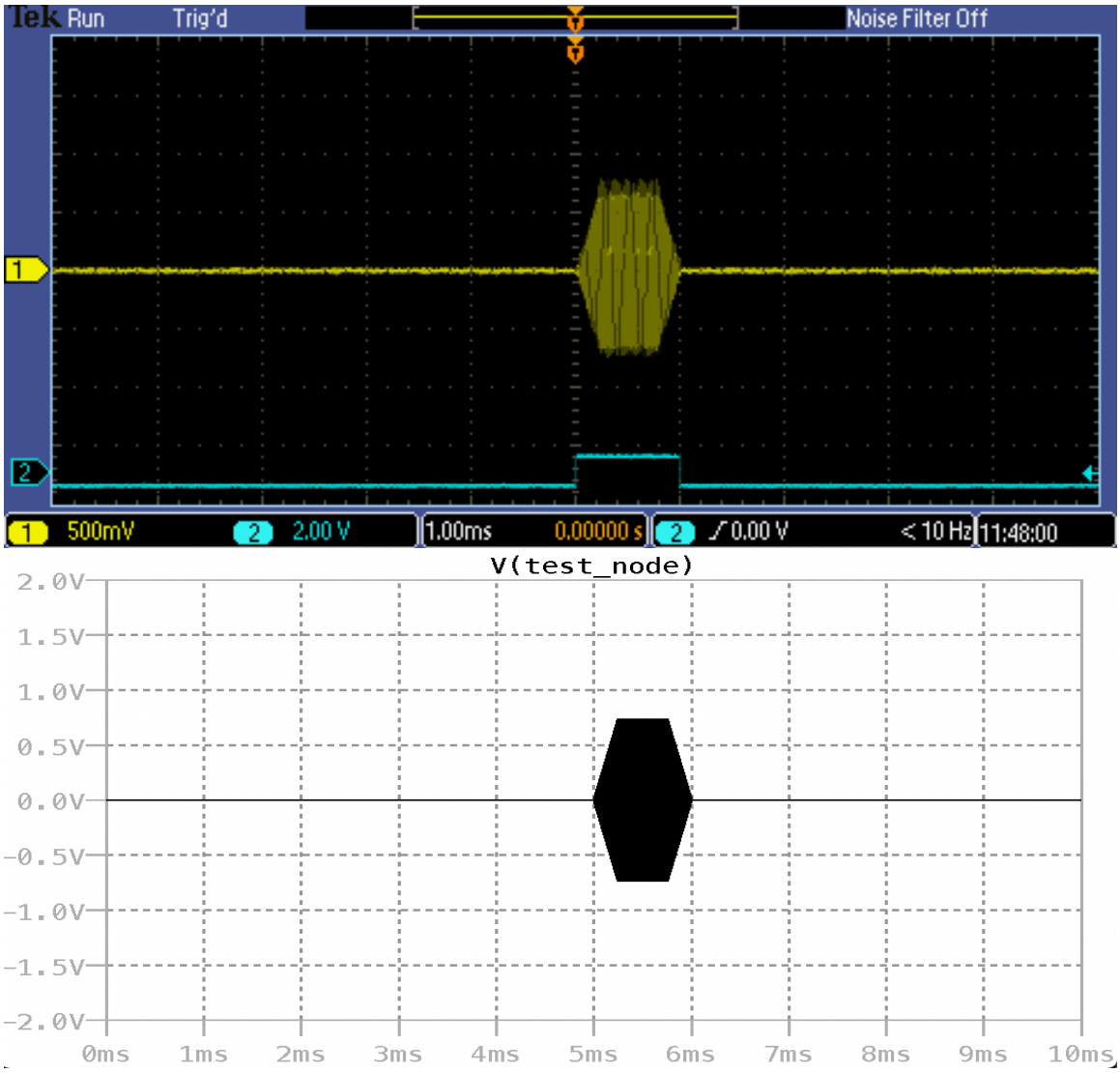

Figure 36. Magnetic field injection – oscillograph(top) and LTspice results(bottom) with jumpers J4 and J5 inserted

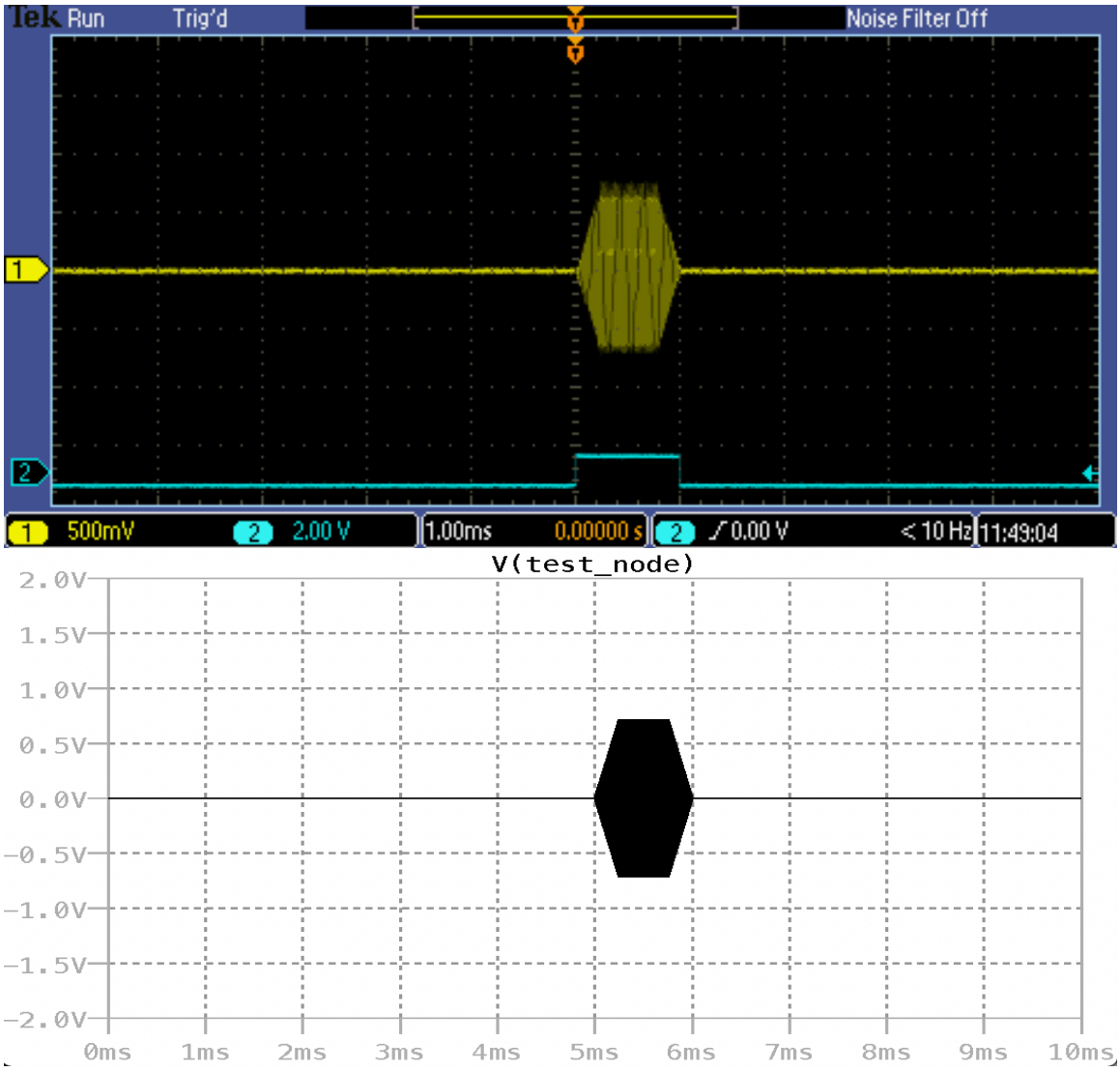

Figure 37. Magnetic field injection – oscillograph(top) and LTspice results(bottom) with jumpers J2, J4, and J5 inserted

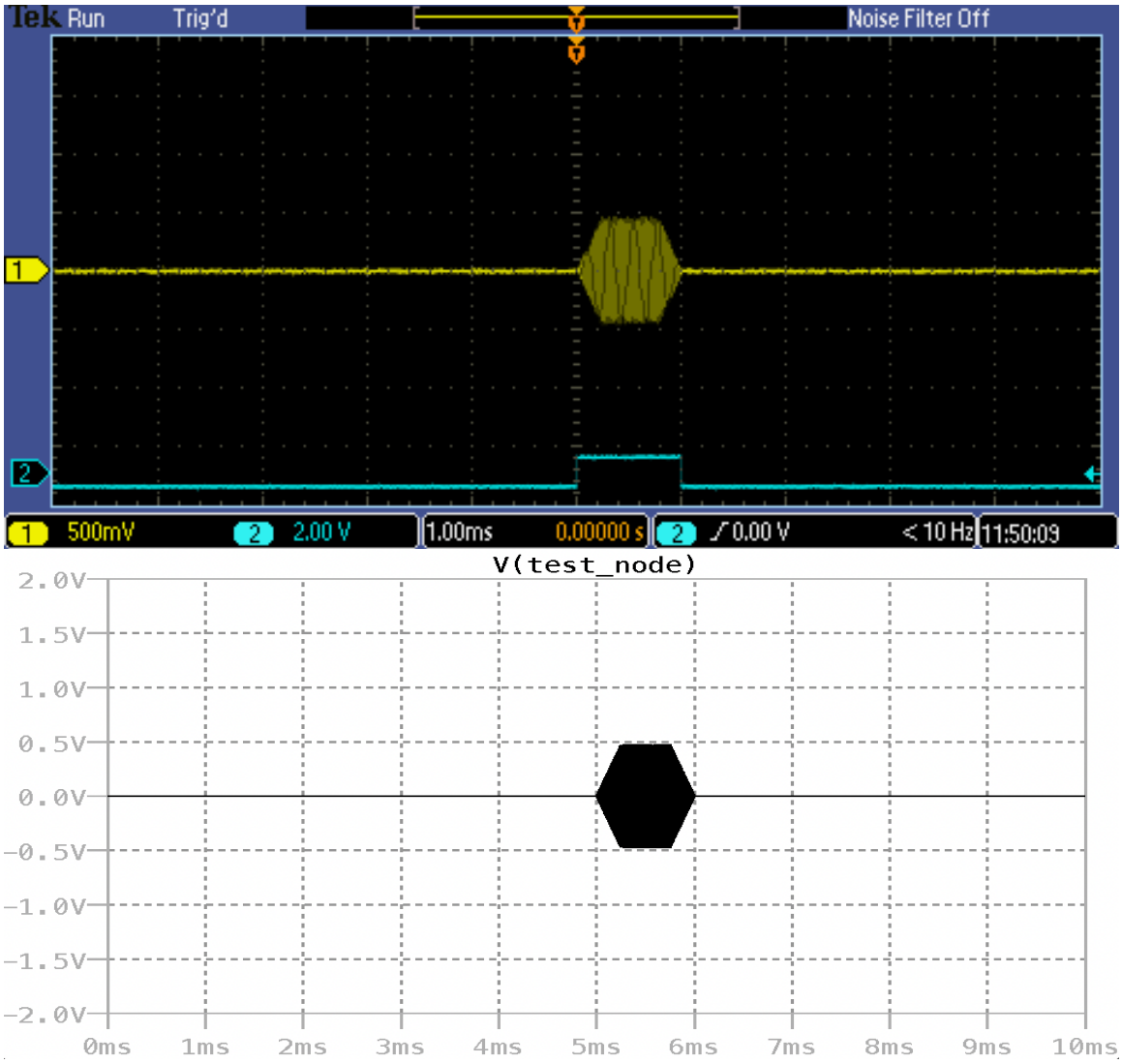

Figure 38. Magnetic field injection – oscillograph(top) and LTspice results(bottom) with jumpers J1, J4, and J5 inserted

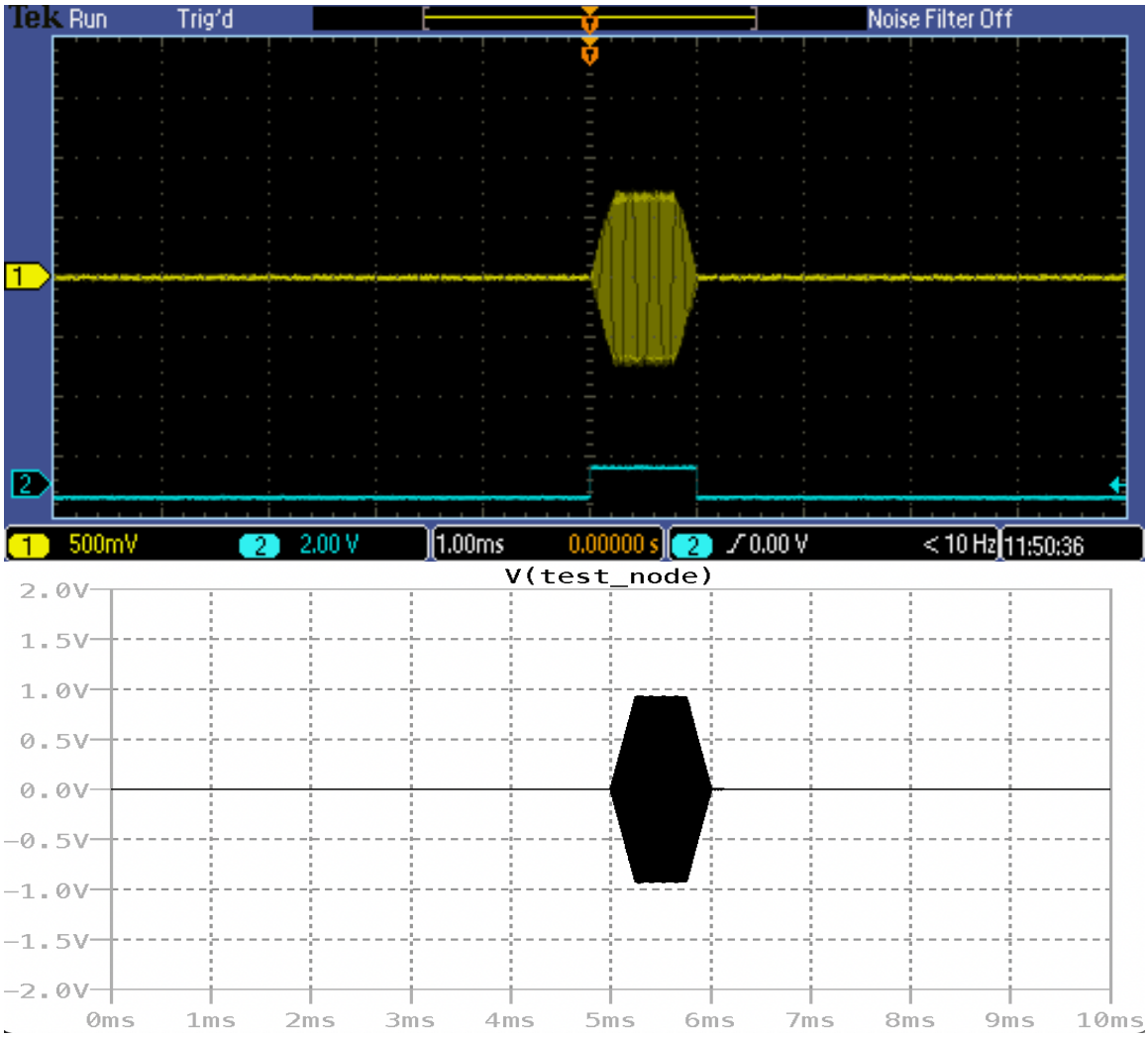

Figure 39. Magnetic field injection – oscillograph(top) and LTspice results(bottom) with jumpers J1, J3, and J5 inserted

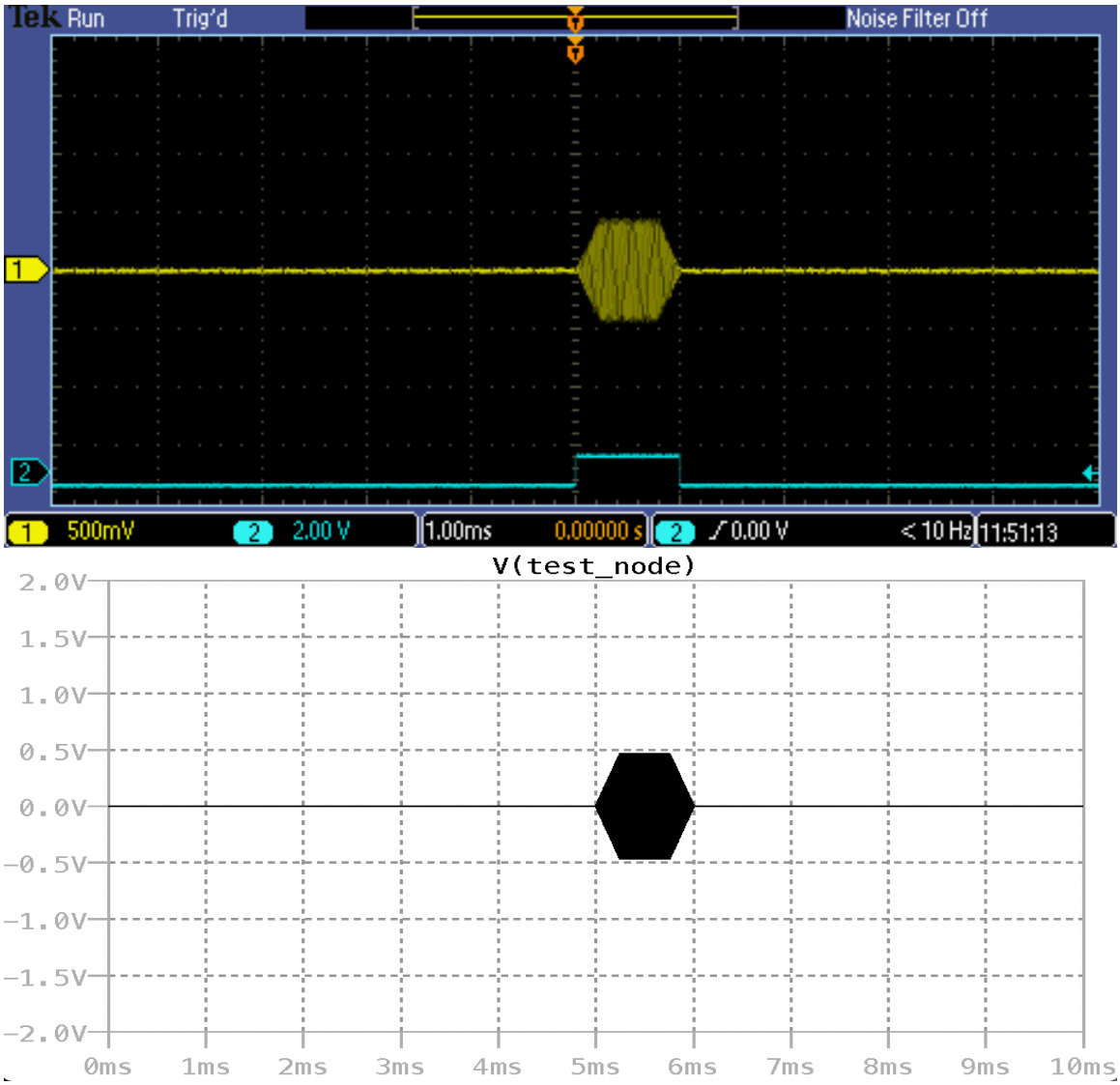

Figure 40. Magnetic field injection – oscillograph(top) and LTspice results(bottom) with jumpers J1, J2, J4, and J5 inserted

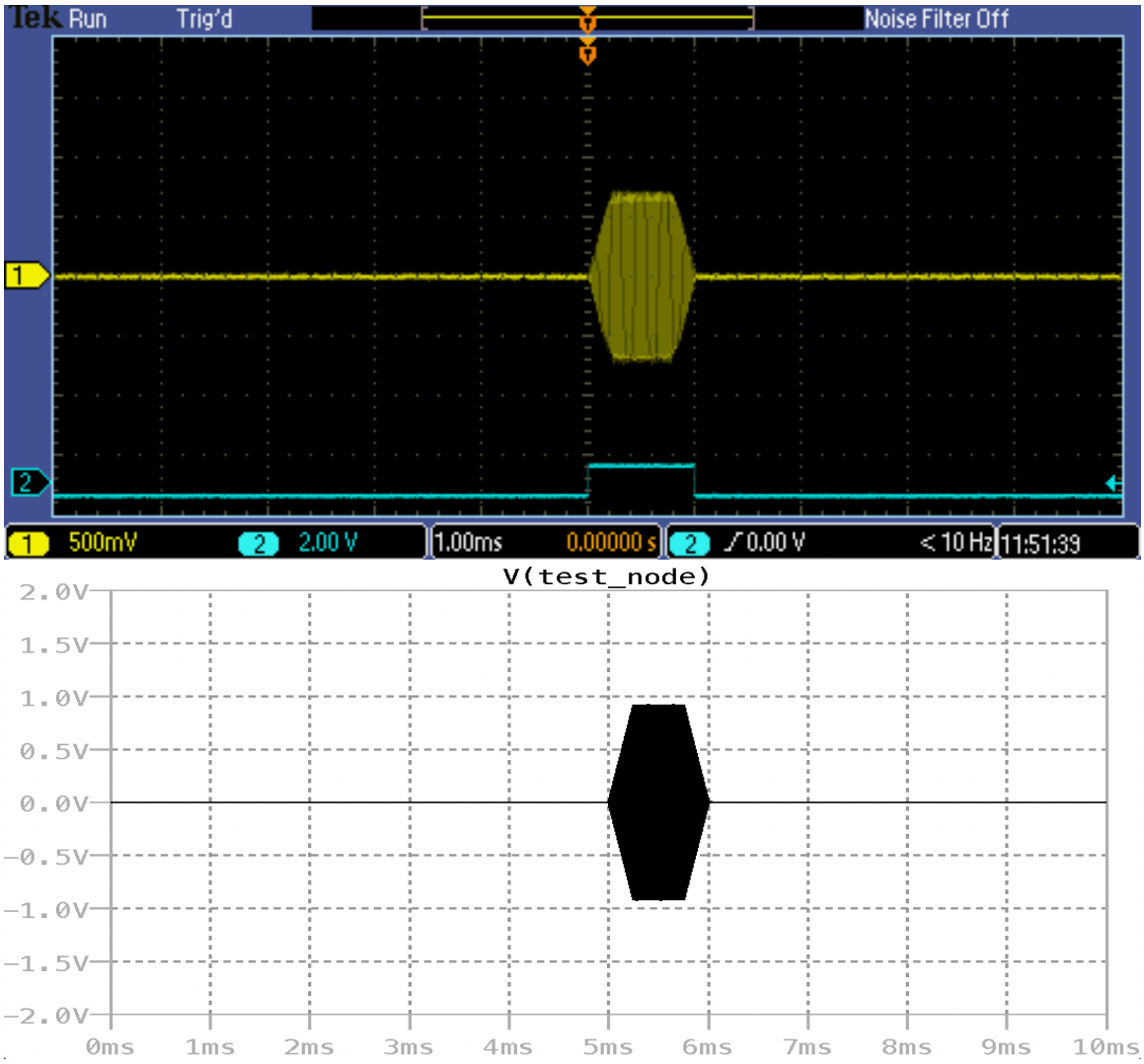

Figure 41. Magnetic field injection – oscillograph(top) and LTspice results(bottom) with jumpers J1, J2, J3, and J5 inserted

From the figures, notice the changes in voltage as different jumper combinations were installed. The voltage was attenuated by adding resistors and a capacitor. These types of filters represent a technique engineers can use to redesign a circuit board that is susceptible to magnetic field coupling [24].

We then repeated the test while the frequency is increased to 4.1 MHz. This frequency is selected to not aliasing with the oscilloscope sampling frequency. Table 7 displays the results of doubling the injection waveform modulated frequency to 4.1 MHz.

Table 7. Results for magnetic field injection testing at frequency = 4.1 MHz and amplitude = 1.0 Vpk

Operating Conditions:	Jumper Configuration:					Results:		
Magnetic Field Freq: 4.1 MHz Amp: 1.0 Vpk	J1	J2	J3	J4	J5	Results (mVpk)	Reference Figure Number	LTspice Results (mVpk)
	EMC test probe					1100		N/A
				x	x	850		830
			x		x	850		830
			x	x	x	850		830
No path		x			x	0		N/A
		x		x	x	850		790
		x	x		x	900		850
		x	x	x	x	900		850
No path	x				x	0		N/A
	x			x	x	320		310
	x		x		x	2100		2600
	x		x	x	x	2100		2600
No path	x	x			x	0		N/A
	x	x		x	x	320		310
	x	x	x		x	2100		2600
	x	x	x	x	x	2100		2600
Ground Reference	x	x	x	x	x	2100	No Change	2600

From the results summarized in Table 7, it is clear that doubling the frequency also doubles the induced voltage. This verifies the theory presented in Chapter II of this thesis and confirms that circuit boards become more susceptible to magnetic field coupling at higher frequencies. One of the benefits of near field injection testing is that the amplitude and frequency of the injected waveform can be quickly controlled by the user to see how the system will respond. Also, the low duty cycle ensures a high level of instantaneous energy, but low average power. This ensures the test are nondestructive for the EUT.

C. ELECTRIC FIELD INJECTION TEST RESULTS

For the electric field injection test, we set up the testbed as described in Chapter IV and connect the electric field injector probe (6) to the output of the RF amplifier (3). The oscilloscope probe (8) is connected to the example circuit board, and displays the signal on Channel 1 of the oscilloscope (4). The electric field injection probe (6) will radiate the modulated waveform with a controllable input frequency and amplitude. The test begins with touching the electric field injector probe (6) to the "surface area" on the example circuit board, as shown in Figure 42. Recall, the electric field injector probe acts as one half of a capacitor and the "surface area" is acting as the other half, thus allowing a common mode current to flow into the circuit.

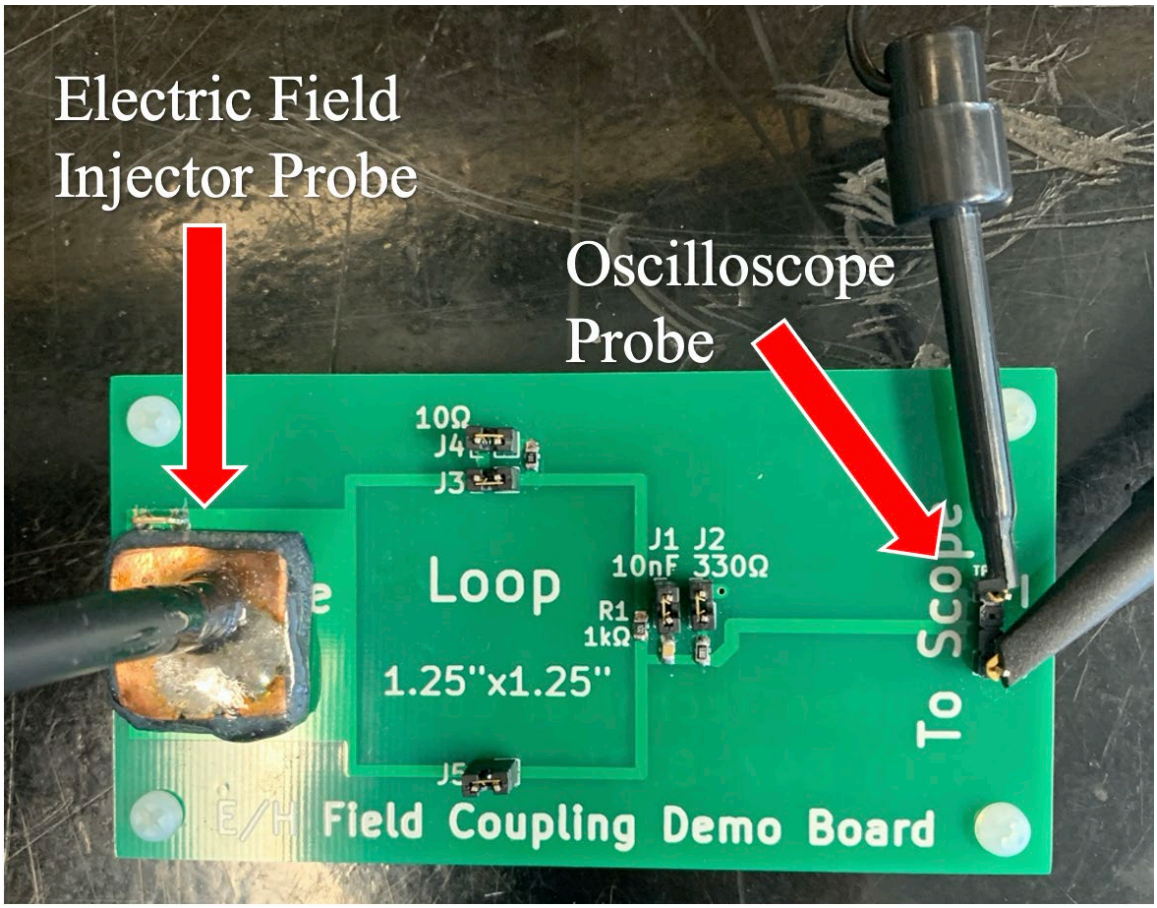

Note: The "Surface Area" can be seen more clearly in Figure 30.

Figure 42. Photograph showing how to apply the electric field injector to the "surface area" of the example circuit board

The electric field probe energy is coupled into the board region labeled “Surface Area.” Applying the electric field injector probe to the “surface area” of the example circuit boards induces a ground referenced common mode current into the system. The equivalent circuit for electric field coupling is a ground referenced current source. Figure 43 is the equivalent circuit of the example circuit board augmented with a current source to model when the electric field injector probe is applied to the “surface area.”

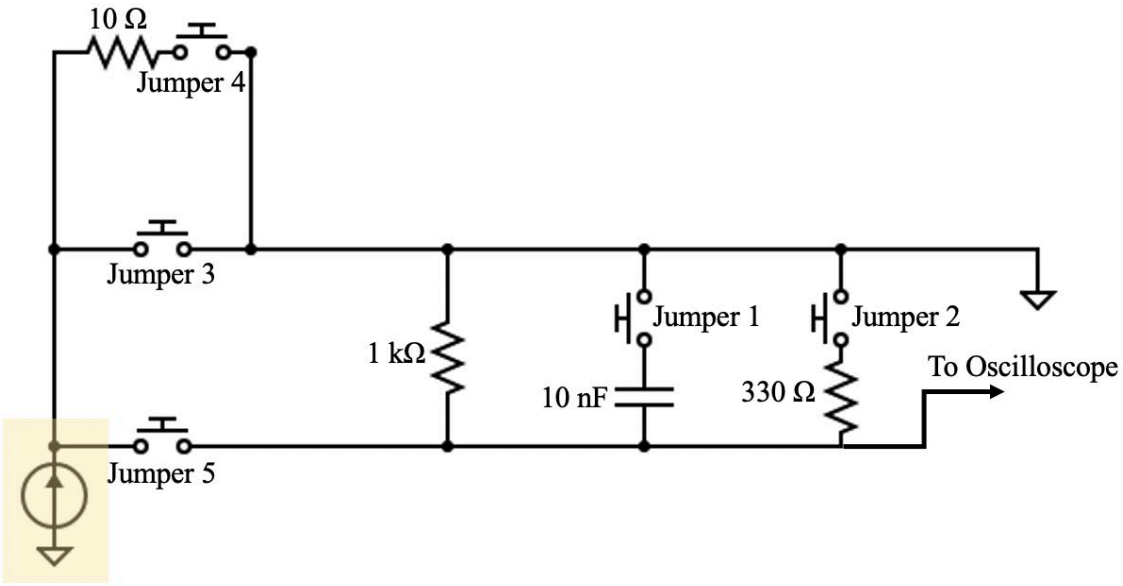

Figure 43. Equivalent circuit drawing of the example circuit board while the electric field injector probe is applied to the board “surface area”

The equivalent drawing shown in Figure 43 is used to model the system using LTspice, so the simulation results can be compared to the experimental test results. Also, in Figure 43, notice the location of the ground reference current source. Jumper 5 must be inserted to allow current to flow to the ground located in the top-right corner of the drawing, Therefore, for all electric field injector testing conducted on the example circuit board, Jumper 5 is inserted.

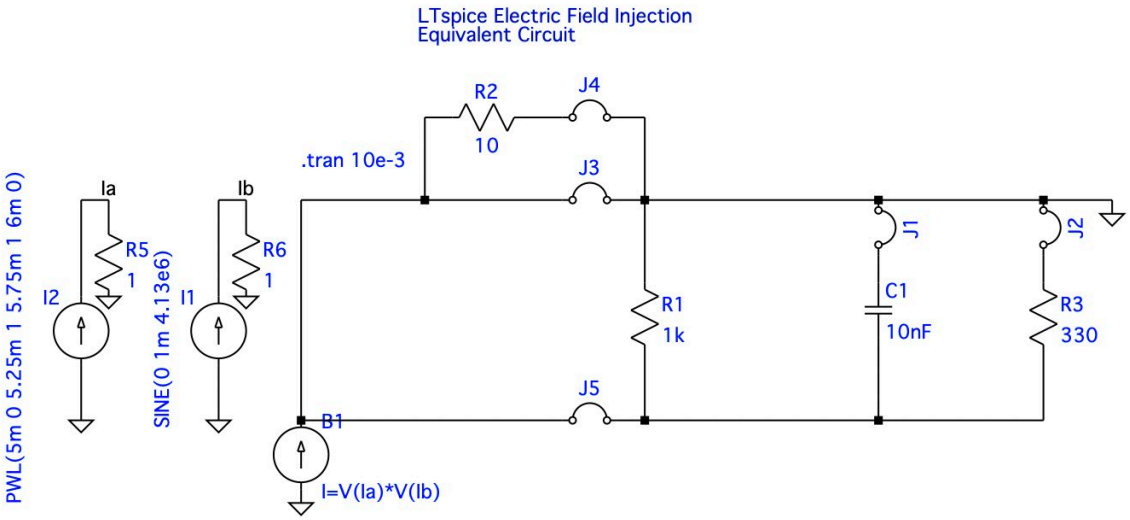

Figure 44. LTspice electric field injection equivalent circuit drawing

Table 8 summarizes the results of testing the example circuit board with an input frequency of 4.1 MHz and amplitude of 1.0 Vpk with multiple jumper configurations. The results of the LTspice simulation are also listed in Table 8.

Table 8. Results of electric field injection testing conducted at a frequency = 4.1 MHz and amplitude = 1.0 Vpk

Operating Conditions:	Jumper Configuration:					Results:		
Electric Field Freq: 4.1 MHz Amp: 1.0 Vpk	J1	J2	J3	J4	J5	Results (mVpk)	Reference Figure Number	LTspice Results (mVpp):
					x	1000	Figure 45	1000
				x	x	15		10
			x		x	< 10		0.1
			x	x	x	< 10		0.1
		x			x	300	Figure 46	247
		x		x	x	15		10
		x	x		x	< 10		0
		x	x	x	x	< 10		0
	x				x	< 10	Figure 47	3.3
	x			x	x	< 10		3
	x		x		x	< 10		0
	x		x	x	x	< 10		0
	x	x			x	< 10		3.3
	x	x		x	x	< 10		3.2
	x	x	x		x	< 10		0
	x	x	x	x	x	< 10		0
Ground Reference					x	0		0
Ground Reference		x			x	0		0
Ground Reference		x		x	x	0		0

Figure 45 through Figure 47 show the oscillographs and LTspice simulation for the test results in Table 8. Notice how the input voltage is 1.0 Vpk, but the resulting voltage when only J5 is inserted is 1000 mVpk. This proves the theory previously stated: the electric field injector acts like a ground reference common mode current source. While J5 in inserted, the current flows form the ground referenced current source, through J5 and the 1 kΩ resistor, and is then measured by the oscilloscope.

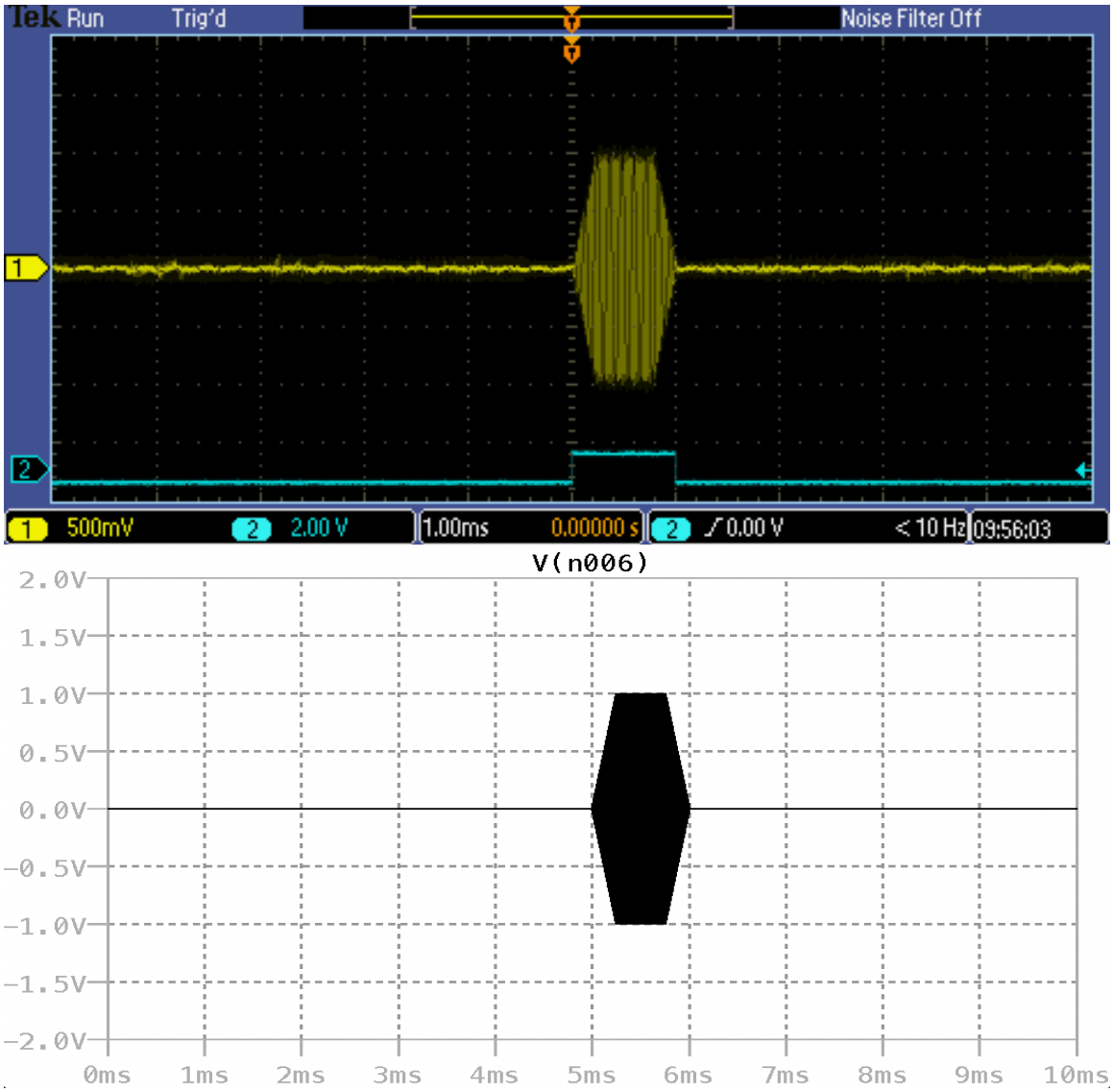

Figure 45. Electric field injection – oscillograph(top) and LTspice results(bottom) with jumper J5 inserted

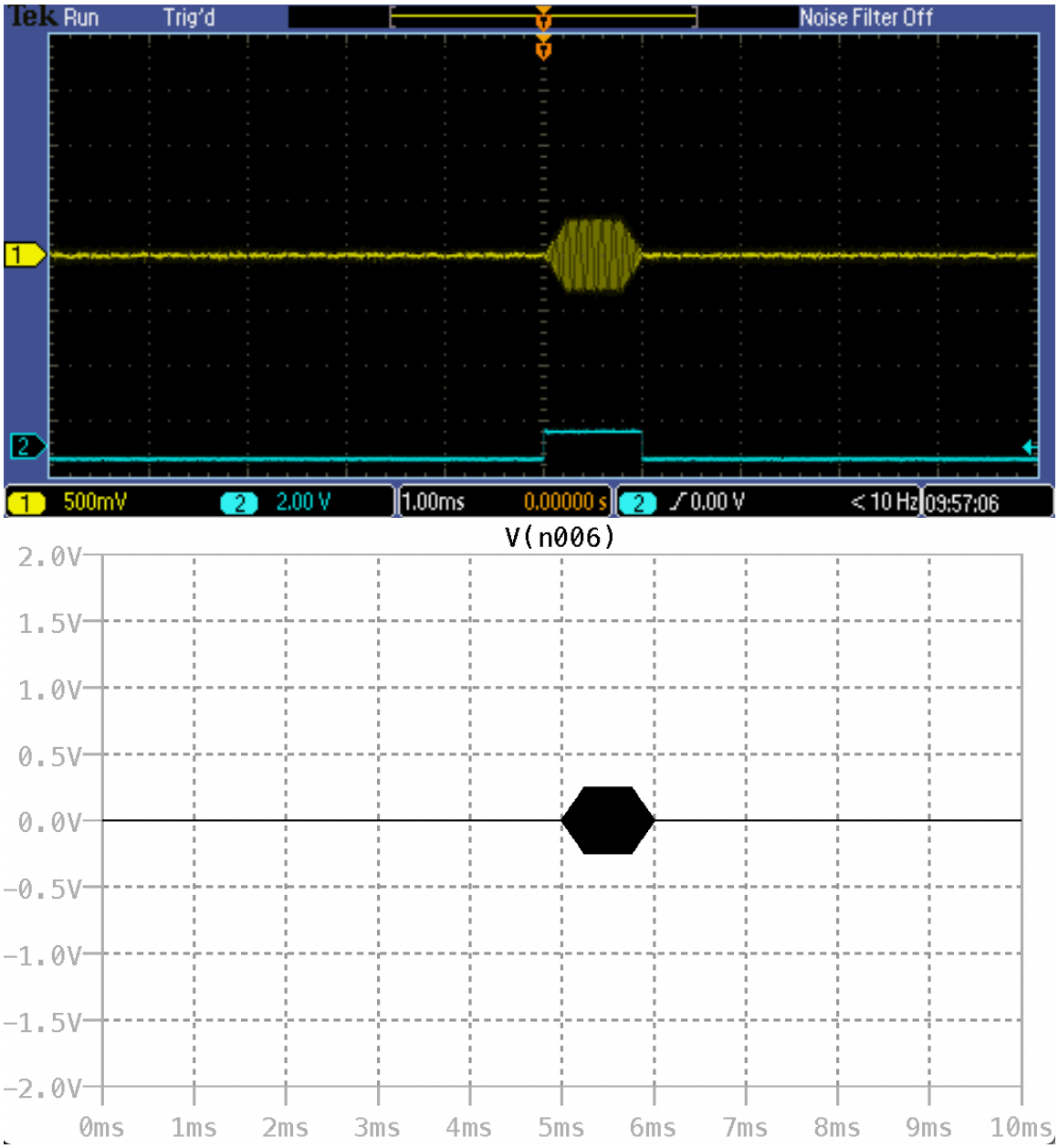

Figure 46. Electric field injection – oscillograph(top) and LTspice results(bottom) with jumpers J2 and J5 inserted

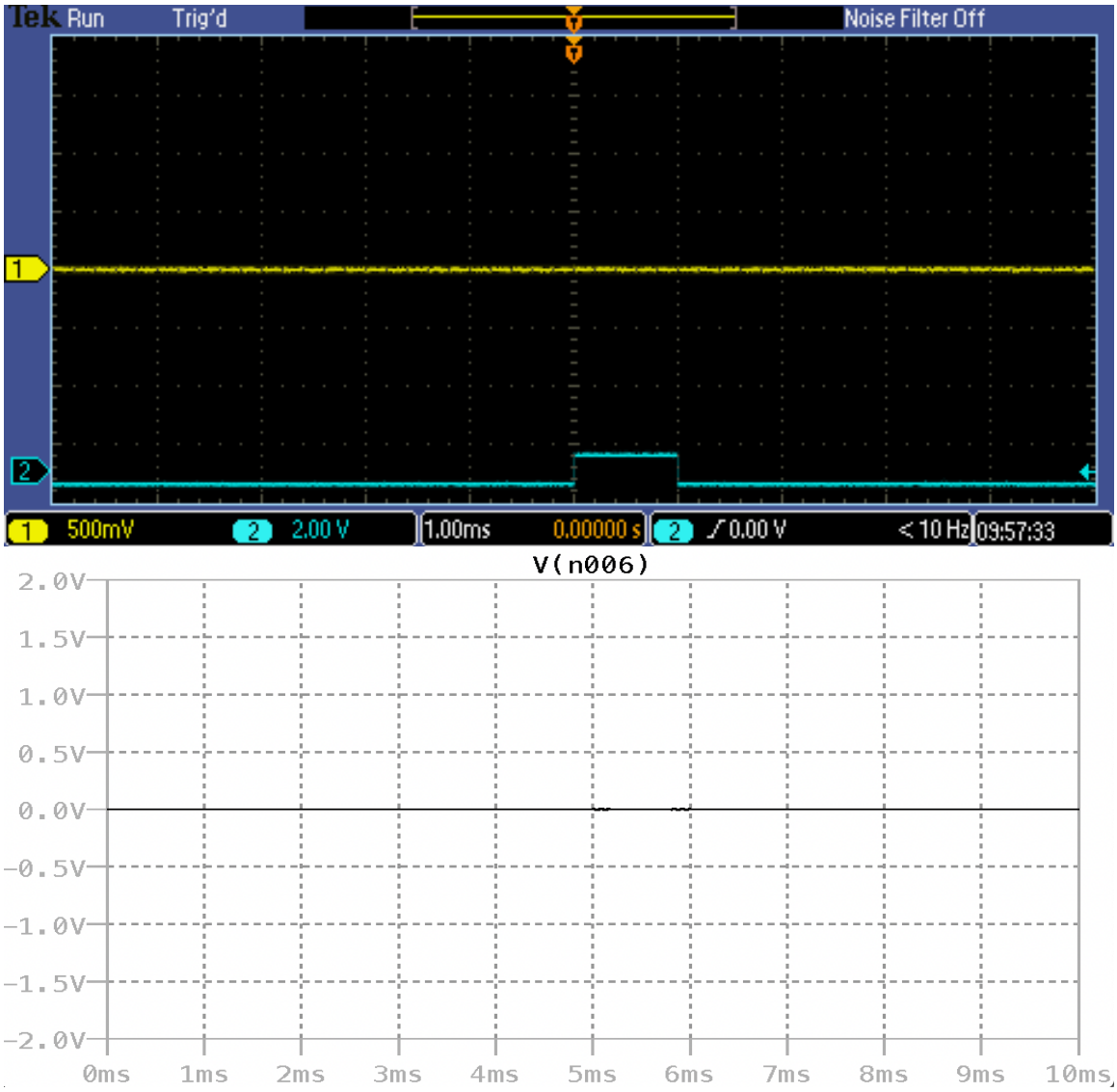

Figure 47. Electric field injection – oscillograph(top) and LTspice results(bottom) with jumpers J1 and J5 inserted

D. DISCUSSION

The test results presented in this chapter match the theory previously presented and the simulated results obtained with LTspice models. The ability to couple electric and magnetic fields into a system using the testbed and test procedures has been confirmed with the results shown above. Therefore, the feasibility of the testbed has been proven.

THIS PAGE INTENTIONALLY LEFT BLANK

VI. CONCLUSION AND FUTURE WORK

A. CONCLUSION

This thesis describes a new method to safely inject the high transient low duty cycle event that occurs within electrical systems, to test the EMI susceptibility of a circuit board. A nondestructive testbed was constructed at NPS to examine the effects of radiated magnetic and electric fields on electrical components. The testbed allows the injection of radiated fields into an EUT using custom built, small, near-field injection probes. One test probe is used to radiate magnetic fields and the other probe is used to radiate electric fields. An example circuit board was tested for EMI susceptibility to measure its response to external electric and magnetic fields. The goal of the test is to couple electric and magnetic fields using the near field test probes and pinpoint the components that are susceptible to electric or magnetic fields. The frequency and amplitude of the injected fields can be controlled by the user.

EMI theory was discussed in Chapter II to present the reader different EMI coupling methods that can induce a voltage or current within a system. Then the test results were verified using Faraday's Law and Ampere's Law. Lastly, the example circuit boards were simulated in LTspice to further confirm the test results were accurate. Chapter II also describes why shielding is not an effective solution to many EMI susceptibility issues.

The FLASH solid state circuit breaker specifications and related EMI challenges were discussed in Chapter III. A detailed description of the FLASH system requirements was presented. Also, the logic boards that will be susceptible to EMI were shown. The possible methods EMI may be coupled into the FLASH solid state circuit breaker were outlined. Lastly, the rational for EMI susceptibility testing and why it is necessary for the FLASH system and other future systems were discussed.

A detailed description and list of required equipment needed to construct the testbed was provided in Chapter IV. The radiated waveform needed to generate a high level of instantaneous energy and low average power was also described. The shape and duty cycle of the radiated waveform were key design components for this thesis because it enables the

test to be nondestructive to the EUT. This provides significant benefits over the traditional EMI susceptibility testing methods, which were often costly and provided less information about the "weak points" of the system.

Chapter V confirmed the theory discussed in Chapter II by testing a prototype circuit boards using this testbed. This validated the theory that magnetic field coupling induces a differential mode voltage, and the electric field injector induced a ground referenced common mode current into the EUT. The impact of the radiated fields could then be reduced in the example circuit boards by adding capacitors and/or resistors. Therefore, proving the EUT was susceptible to EMI through magnetic and electric field coupling, and then attenuated by implementing different fixes.

B. FUTURE WORK

To continue the research that was started in this thesis, more equipment is needed. For example, a working logic board designed for the FLASH circuit breaker and the higher bandwidth RF power amplifier listed in Table 2. The logic boards are still in the prototyping phase and not ready for testing, and the RF power amplifier has not yet arrived at NPS. Due to the lack of these items, representative testing on an evaluation board was conducted to verify the operation of the testbed. However, the testbed designed in this thesis can be used to test any circuit board that may be exposed to a hostile EMI environment or may be susceptible to EMI.

Another student at NPS will be continuing this research for the next year. The goal of his research will be to use the testbed and procedures described in this thesis to test the FLASH logic circuit board for EMI susceptibility. Upon successful testing of the system, this student will propose improvement methods to the logic board designers to make the system more robust in its EMI environment. This will ensure the FLASH program can meet all specifications required by NASA and not fail due to EMI susceptibility. Designing and testing the logic board to be resilient in an EMI environment also reduces the need for expensive and heavy filtering or shielding.

LIST OF REFERENCES

[1] M. Schutten, Seminar, Topic "EMI: Theory, Coupling, Mechanisms, Equivalent Circuits, and Solutions." GE Global Research, Jul. 26, 2011.

[2] E. Orietti, N. Montemezzo, S. Buso, G. Meneghesso, A. Neviani and G. Spiazzi, "Reducing the EMI susceptibility of a Kuijk bandgap," in *IEEE Transactions on Electromagnetic Compatibility*, vol. 50, no. 4, pp. 876–886, Nov. 2008, doi: 10.1109/TEMC.2008.2004581.

[3] C. Fu, J. Zhou, X. Zhang and C. Cui, "Electromagnetic compatibility design of intelligent circuit breaker," *2011 Third International Conference on Measuring Technology and Mechatronics Automation*, 2011, pp. 19–21, doi: 10.1109/ICMTMA.2011.292.

[4] Paul, C. R. (2006). I*ntroduction to Electromagnetic Compatibility*. Hoboken, NJ: Wiley-Interscience.

[5] M. Schutten, "EMI susceptibility testing apparatus and methods" U.S. Patents 6242925 B1, Jun. 5, 2001 [Online]. Available: https://patft.uspto.gov/netacgi/nph-Parser?Sect1=PTO1&Sect2=HITOFF&d=PALL&p=1&u=%2Fnetahtml%2FPTO%2Fsrchnum.htm&r=1&f=G&l=50&s1=6242925.PN.&OS=PN/6242925&RS=PN/6242925

[6] Requirements for the Control of Electromagnetic Interference Characteristics of Subsystems and Equipment, MIL-STD-461G, Dec. 2015. [Online]. Available: https://www.atecorp.com/atecorp/media/pdfs/data-sheets/mil-std-461g.pdf

[7] D. Zhang "Fast light-weight altitude-ready solid-state circuit breaker for hybrid electric propulsion (FLASH) white paper." Naval Postgraduate School, Monterey, CA. Accessed: Sep. 15, 2021.

[8] W. Smith, "Loose radar blips nearly sink ships," *The Courier Mail,* Feb. 1, 2002.

[9] K. Armstrong, "The First 855 "Banana Skins"," *EMC Journal*, 2014 [Online]. Available: https://www.nutwooduk.co.uk/pdf/banana%20skins.pdf

[10] *Electromagnetic Environmental Effects Requirements for Systems,* MIL-STD-464, Version C, Dec. 2010. [Online]. Available: http://everyspec.com/MIL-STD/MIL-STD-0300-0499/MIL-STD-464C_28312/

[11] M. L. Evans "USS Forrestal (CV-59)." Dictionary for the American Naval Fighting Ship, Sep. 11, 2017 [Online]. Available: https://www.history.navy.mil/research/histories/ship-histories/danfs/f/forrestal-cva-59.html

[12] W. Pentland, “Yes, our gadgets really threaten planes.” *Forbes*, Sep. 10, 2012 [Online]. Available: https://www.forbes.com/sites/williampentland/2012/09/10/yes-our-gadgets-really-threaten-planes/?sh=3b73c4fe3599

[13] H.W. Ott, “Digital circuit radiation,” in *Electromagnetic Compatibility Engineering*, Hoboken, NJ, USA: John Wiley & Sons, Inc., 2009, ch. 12, sec. 1–3, pp. 464–481.

[14] S. Blanchette, J. R. Bray and Y. M. M. Antar, “Development and Evaluation of Waveforms for EMI Radiated Susceptibility Testing of Avionic Systems,” *2018 IEEE Symposium on Electromagnetic Compatibility*, Signal Integrity and Power Integrity (EMC, SI & PI), 2018, pp. 24–29, doi: 10.1109/EMCSI.2018.8495365.

[15] R. Hoad, N. J. Carter, D. Herke and S. P. Watkins, “Trends in EM susceptibility of IT equipment,” in *IEEE Transactions on Electromagnetic Compatibility*, vol. 46, no. 3, pp. 390–395, Aug. 2004, doi: 10.1109/TEMC.2004.831815.

[16] B. Adamczyk, “Conducted emissions measurements: Voltage method,” *In Compliance,* Jul. 31, 2017. [Online]. Available: https://incompliancemag.com/article/conducted-emissions-measurements-voltage-method/

[17] L. A. Mallette and R. Adams, “An introduction of EMI/EMC test requirements for space application,” *1999 IEEE Aerospace Conference.* Proceedings (Cat. No.99TH8403), 1999, pp. 213–221 vol.5, doi: 10.1109/AERO.1999.790203.

[18] D. Fleisch, *A Student’s Guide to Maxwell’s Equations,* Cambridge Univ. Press, Cambridge, U.K., 2008.

[19] *Manual of Regulation and Procedures for Federal Radio Frequency Management*, May 2013 ed., Nat. Telecommun. and Inf. Admin., Washington, DC, 2017, pp 3–6 – 3–9.

[20] Yaping Du, T. C. Cheng and A. S. Farag, “Principles of power-frequency magnetic field shielding with flat sheets in a source of long conductors,” in IEEE Transactions on Electromagnetic Compatibility, vol. 38, no. 3, pp. 450–459, Aug. 1996, doi: 10.1109/15.536075.

[21] *Grounding, Bonding, And Shielding for Electronic Equipments and Facilities*, MIL-HSBK-419, Version A, Dec. 29, 1987 [Online]. Available: https://www.wbdg.org/FFC/NAVFAC/DMMHNAV/hdbk419a_vol1.pdf

[22] B. D. Russell, W. C. Kotheimer and R. lIalewski, “Substation Electromagnetic Interference Part 2: Susceptibility Testing and EMI Simulation in High Voltage Laboratories,” in *IEEE Transactions on Power Apparatus and Systems*, vol. PAS-103, no. 7, pp. 1871–1878, July 1984, doi: 10.1109/TPAS.1984.318651.

[23] F. Grassi, G. Spadacini, F. Marliani and S. A. Pignari, “Use of Double Bulk Current Injection for Susceptibility Testing of Avionics,” in *IEEE Transactions on Electromagnetic Compatibility*, vol. 50, no. 3, pp. 524–535, Aug. 2008, doi: 10.1109/TEMC.2008.926810.

[24] E. Orietti, N. Montemezzo, S. Buso, G. Meneghesso, A. Neviani and G. Spiazzi, “Reducing the EMI Susceptibility of a Kuijk Bandgap,” in *IEEE Transactions on Electromagnetic Compatibility,* vol. 50, no. 4, pp. 876–886, Nov. 2008, doi: 10.1109/TEMC.2008.2004581.

THIS PAGE INTENTIONALLY LEFT BLANK

INITIAL DISTRIBUTION LIST

1. Defense Technical Information Center
   Ft. Belvoir, Virginia

2. Dudley Knox Library
   Naval Postgraduate School
   Monterey, California